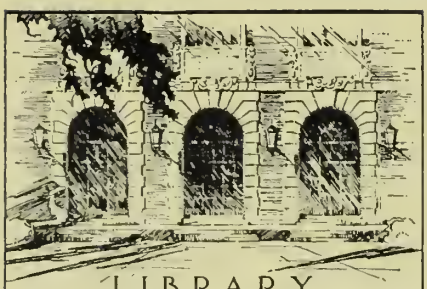

ANTENNA LABORATORY

Technical Report No. 47

LOGARITHMICALLY PERIODIC RESONANT-V ARRAYS

by

Paul E. Mayes and Robert L. Carrel

15 July 1960

Contract AF33(616)-6079
Project No. 9-(13-6278) Task 40572

Sponsored by:

WRIGHT AIR DEVELOPMENT CENTER

Electrical Engineering Research Laboratory
Engineering Experiment Station
University of Illinois
Urbana, Illinois

CONTENTS

1. INTRODUCTION

The principle of logarithmic periodicity has become well-established in the design of frequency independent antennas. The first log-periodic antennas had moderate directive gain. Like the logarithmic spiral[1,2] antennas, however, the log-periodic structures were unusual because they maintained nearly the same value of gain over arbitrary frequency bands. In order to achieve higher gains log-periodic antennas have been used in arrays and as feeds for reflectors and lenses[3,4]. The purpose of this paper is to show that higher gains are also obtainable with operation of LP antennas in higher order modes.

The log-periodic principles have recently been applied to the design of a frequency independent array of dipoles[5]. By proper choice of design parameters, the log-periodic dipole array with a length of the order of one wavelength at the lowest frequency can be made to yield a directive gain of 10 db (compared to an isotropic radiator) over a 2:1 bandwidth. Lower gains can be achieved over much wider bandwidths. The pattern and impedance are essentially independent of frequency over a bandwidth which is governed by the size of the structure and the precision of construction.

The directivity of the log-peridoic dipole array is achieved from both the directive element pattern of the half wave dipoles and the directive array factor of an end-fire array. The directivity can be increased by replacing the half-wave dipoles with more directive resonant-V elements. To obtain the increased directivity of the V elements it is necessary to operate the elements at higher odd-half-wavelength resonances. Directive gains in excess of 15 db over isotropic can be achieved when operating the array in the higher modes. The same structure can be used in several modes to achieve coverage of different frequency bands. An efficient utilization of the structure is obtained in this way, since many of the elements will be used at more than one frequency.

Typical directive gains from 12 db (over isotropic) in the three-half-wavelengths mode to 17 db in the seven-half-wavelengths mode have been obtained. The input impedance can be controlled to some extent by choice of design parameters. A VSWR less than 3:1 can be achieved across

the entire band covered by several modes except at "transition" regions where operation changes from one mode to another.

2. DEVELOPMENT OF THE LOG-PERIODIC RESONANT-V ARRAY

2.1. Log-Periodic Design Principles

2.1.1 Similitude

The idea in log-peridoic antenna design is to use the principle of similitude[6] in the design of interconnected "cells" of the antenna. Each cell is exactly like the adjacent cell except for a scale factor, τ. Such a connected group of cells is shown schematically in Figure 1. If the number of cells is unlimited, the entire structure will transform into itself when scaled by τ or any integer power of τ. It is assumed that the structure is built from very good conductors so that the effect of finite conductivity can be neglected in the application of similitude.

If the method used to excite the structure is independent of frequency, the electromagnetic performance must be the same (except for a change in scale) at all frequencies related by τ^n (n integer). This frequency independent requirement on the excitation dictates that the source be placed at the small end of the structure.

Each band of frequencies between any f and τf corresponds to one period of the structure. In order to be frequency independent (or nearly so) the variation in performance across a frequency period must be negligible. Not all log-periodic structures are frequency independent antennas. There are a number of log-periodic structures, however, which, for a limited range of parameters, do display only a small variation in performance over a period.

2.1.2 Truncation

In any physical structure it is possible to duplicate the conditions outlined above only for a finite (relatively small) number of cells. Since each successive cell must be increasingly larger, it is inevitable that one must reach a practical limit as to size. Going in the other direction, there is a limit to the precision with which one can construct the very small cells. Therefore, it is necessary to truncate the idealized infinite bandwidth structure to form a practical antenna. If at some frequency most of the energy is radiated from a limited number of cells of the structure, then it is possible that the portion of the structure beyond the radiating section will be unexcited and its presence or absence makes

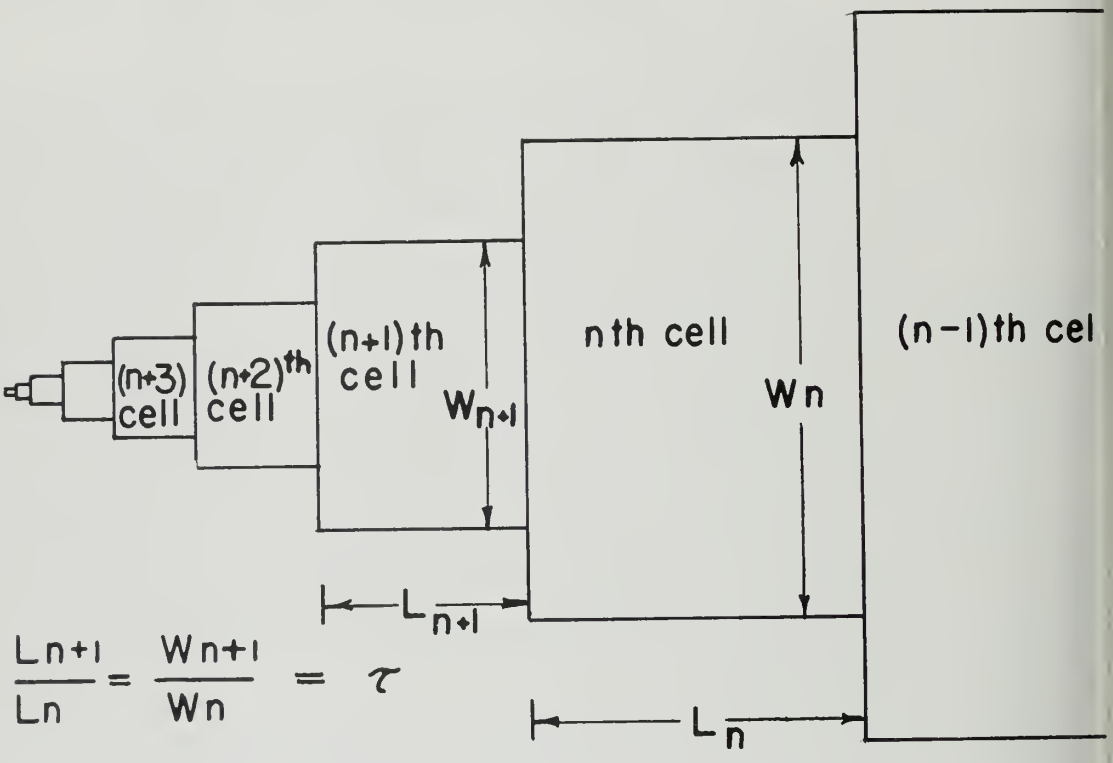

Figure 1. An Interconnection of a Geometrical Progression of Cells which Results in Logarithmically Periodic Performance.

no difference in the electromagnetic performance at this frequency. In this case the fact that the structure has an end rather than extending to infinity will not be observable. The troublesome "end effect" of biconical, discone and similar antennas is thereby eliminated.

2.1.3 The Active Region

From similitude it follows that the radiating portion of the antenna must move along the structure as frequency changes. As frequency decreases the movement will be towards the large end. Ultimately this "active region" will approach the truncation at the large end. When this occurs the antenna will cease to function properly. The low frequency limit of the antenna bandwidth is thus fixed by the position of the truncation on the large end.

As frequency increases the active region moves toward the small end. At the small end there will be a junction region where the feed is attached to the periodic structure. The true periodic geometry can only be carried accurately to a certain point, and beyond this point a transition to the feed geometry must occur. When the active region moves into this transition as frequency increases once again the antenna performance will deteriorate and the high frequency limit on bandwidth will have been reached.

2.2 The Log-Periodic Dipole Array

2.2.1 Description

Isbell found that the log-periodic principles could be applied to the design of an array of half-wave dipoles shown schematically in Figure 2. To be true to the log-periodic principles the diameter of each element should be scaled as well as the length. Also the feed line should be tapered, i.e., a conical line. Strict adherence to these requirements is not necessary, however, as long as the feed line dimension and element diameters remain small in terms of the wavelength over the entire band. In order to obtain radiation toward the small end, and thus avoid exciting the larger elements beyond the active dipoles, π radians phase shift was added between adjacent elements by effectively "twisting" the feeder.

2.2.2 Results

Dipole arrays were found to provide nearly constant patterns and impedance over a band of frequencies which could be extended by adding

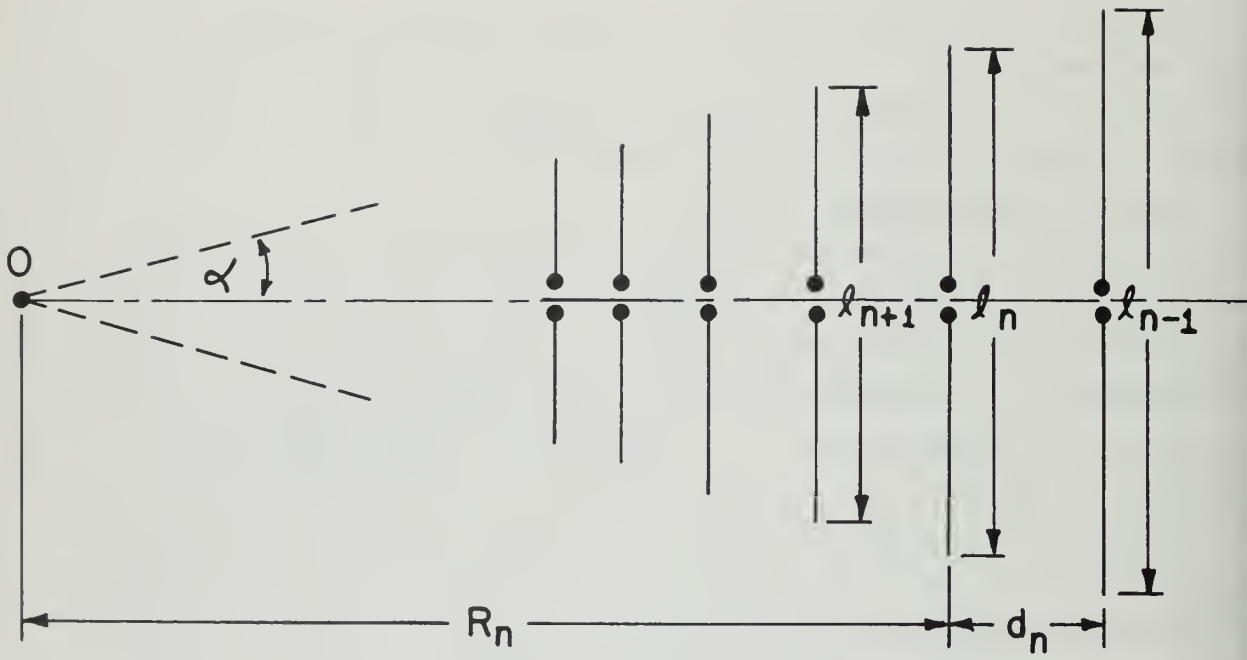

$$\frac{\ell_n}{\ell_{n-1}} = \tau$$

METHOD OF FEEDING

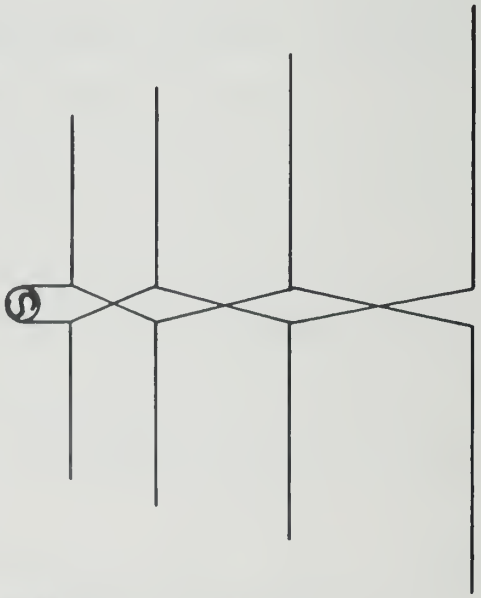

Figure 2. The Log-Periodic Dipole Array

more properly-scaled elements to the structure. It was verified that most of the energy was radiated from the vicinity of the half-wavelength element. With a variation in parameters τ, the scaling factor, and α, the angle defining the ends of the elments, the following trends were found:

(a) the directive gain increases as τ increases and α decreases

(b) the average input impedance level decreases with increasing α and increasing τ.

It has subsequently been found that the impedance of the feed line plays a dominant role in determining the input impedance. It is therefore possible to design log-periodic dipole arrays to meet directivity and impedance specifications within certain limits. Directivities up to 10 db (over isotropic) are easily achieved. Generally speaking, high directivity in a log-periodic antenna implies that the active region is extended over a number of elements which results in a smaller bandwidth than that of an antenna of the same total length but with lower directivity. Impedance levels from 55 to 100 ohms were obtained by Isbell using a feeder with a characteristic impedance of 105 ohms.

The dipole array offers considerable advantage over comparable parastic (Yagi) arrays in bandwidth and as a result is much less critical to adjust for proper operation.

2.3 Theory of Higher Order Resonant Modes

In order to achieve high directivity with the log-periodic dipole array it is necessary to use long thin arrays (small α) or to use an array of two or more dipole arrays. The achievement of satisfactory performance of the dipole array at microwave frequencies is difficult because small tolerances must be met in construction of the very small elements required. The log-periodic array of resonant-V elements offers an alternate way to achieve these desirable characteristics of high directivity and high frequency performance.

An array achieves its directivity from both the element pattern and the array factor of the elements. The LP dipole array makes effective use of the array factor of elements in the active region to achieve end-fire directivity. The element pattern, however, is limited to that of the half-wave dipoles. A similar array of elements having higher directivity

than the half-wave dipole would be desirable for many applications. Of course, the increased directivity would come at the expense of increased element size in terms of wavelength.

The linear dipole possesses resonances at $n\lambda/2$ where n is an integer. Energy is readily accepted from the feeder line of an LP dipole array by dipoles which are near any of the odd-integer resonances (n = 1,3,5,7,etc.). Thus, if an LP dipole array is operated at a wavelength shorter than twice the smallest element length, the energy on the feeder will propagate to the vicinity of the three-half-wavelength element and be radiated. The element patterns of linear dipoles in the higher order resonances are not desirable, however, because they possess multiple lobes as shown in Figure 3. When the conductors are bent into the V-shape, however, the pattern has only two principal lobes with secondary lobes of small magnitude. The array factor of the LP dipole array has displayed good front-to-back ratio so that the backward lobe of the V pattern would not appear appreciably in the pattern of a log-periodic array of resonant-V elements.

Since the input impedance of linear elements near higher order resonances resembles that near the half-wavelength resonance, it would be expected that the input impedance to the array in the higher modes would behave very much like that of the LP dipole array in the $\lambda/2$ mode.

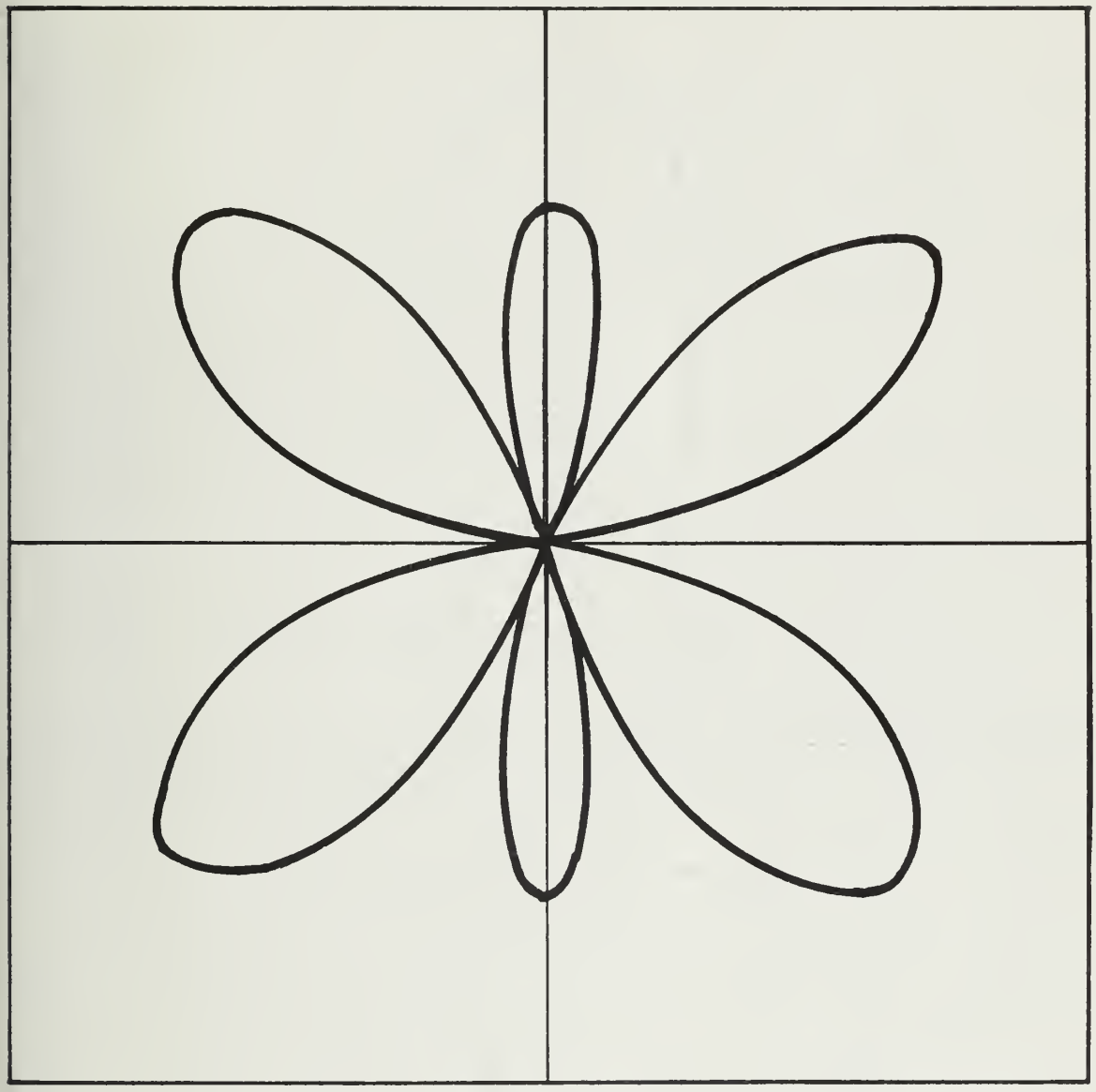

(a) 3 λ/2 LINEAR DIPOLE

Figure 3. E-plane Patterns of Three-Half-Wavelengths Linear Dipole and Resonant-V.

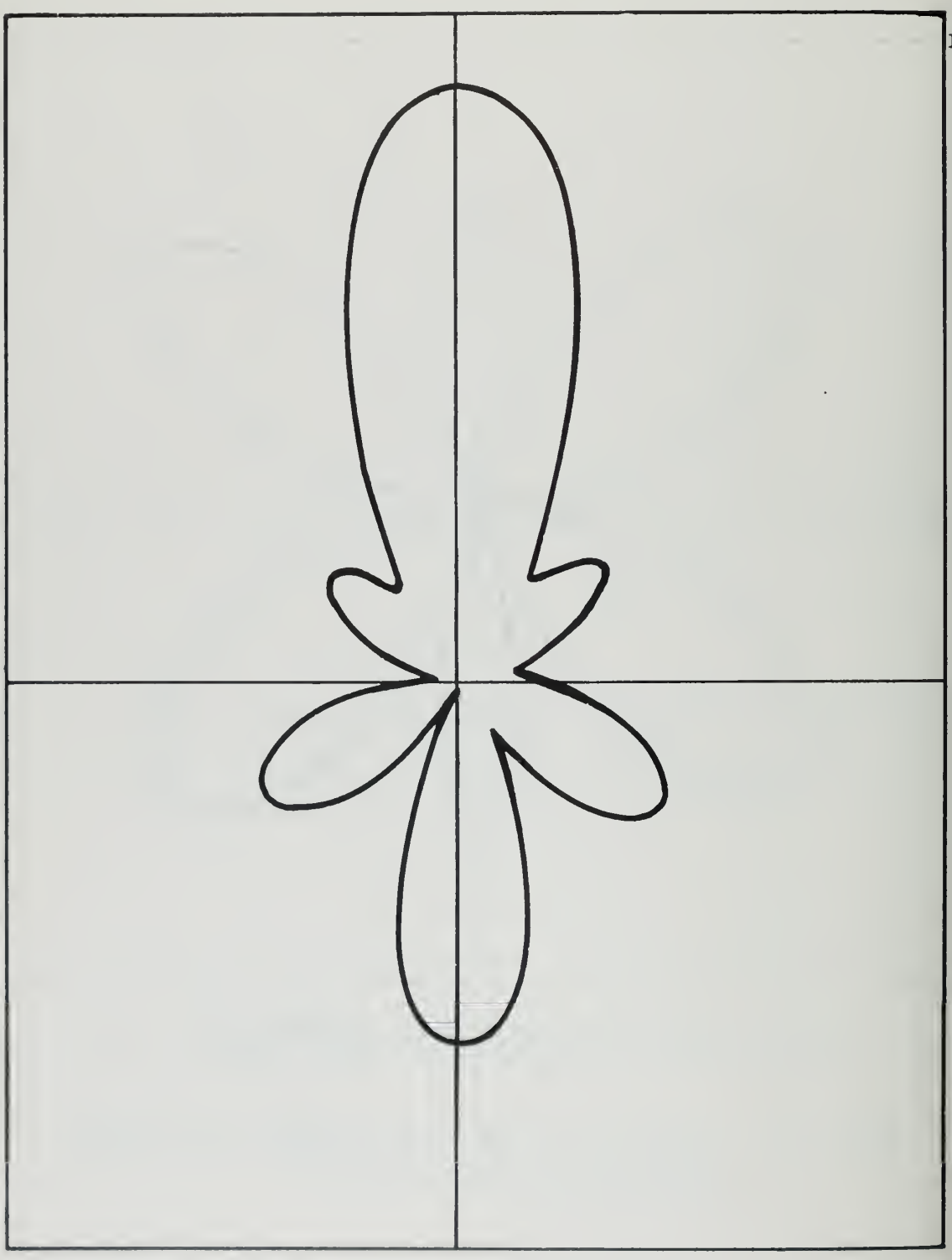

(b) 3λ/2 RESONANT - V

Figure 3b

3. EXPERIMENTAL RESULTS

The reasoning outlined in Section 2.3 was tested in June 1959 by constructing a small model log-periodic V (LPV) array. The initial results were satisfactory and a systematic investigation of LPV antennas with various parameters was undertaken. In addition to the parameters in common with the LP dipole array the LPV array is described by ψ, the angle between the element and the plane normal to the feeder. Figure 4 shows the LPV array schematically.

3.1 Pattern Measurements

3.1.1 Construction of the Pattern Models

The LPV arrays are described by the following parameters (Refer to Figure 4):

τ - The periodic scaling factor

h_1, h_N, - the half lengths of the longest and shortest elements ($\ell = 2h$)

$\sigma = \frac{d_n}{4h_n}$ - the spacing to length ratio

ψ - the angle between the plane normal to the array axis and the V elements.

Z_o - the characteristic impedance of the feeder

a/h - radius to half length ratio of elements

Since α and ψ are not independent parameters in the LPV arrays, the new parameter, σ was defined for these antennas. The parameter σ gives approximately the spacing in wavelengths between elements near the active region in the $\lambda/2$ mode. For the n-th mode the spacing in wavelengths near the active region is approximately $n\sigma$. When α is used with the LPV arrays in the following it will signify the angle which would be subtended by a half element if the element were perpendicular to the feeder rather than bent to form a V. In this sense the parameter α can be used to compare LP dipole and LPV arrays. Given α and τ, σ can be determined from the formula

$$\sigma = \frac{1}{4} [1-\tau] \cot \alpha \qquad (1)$$

A nomograph of this relationship is given in Figure 5.

Several small models of LPV arrays have been constructed for radiation pattern measurements. Coin silver tubing (0.125 in. and 0.148 in. diameter) was used for the feeder conductors and copper wire (0.05 in. diameter) was

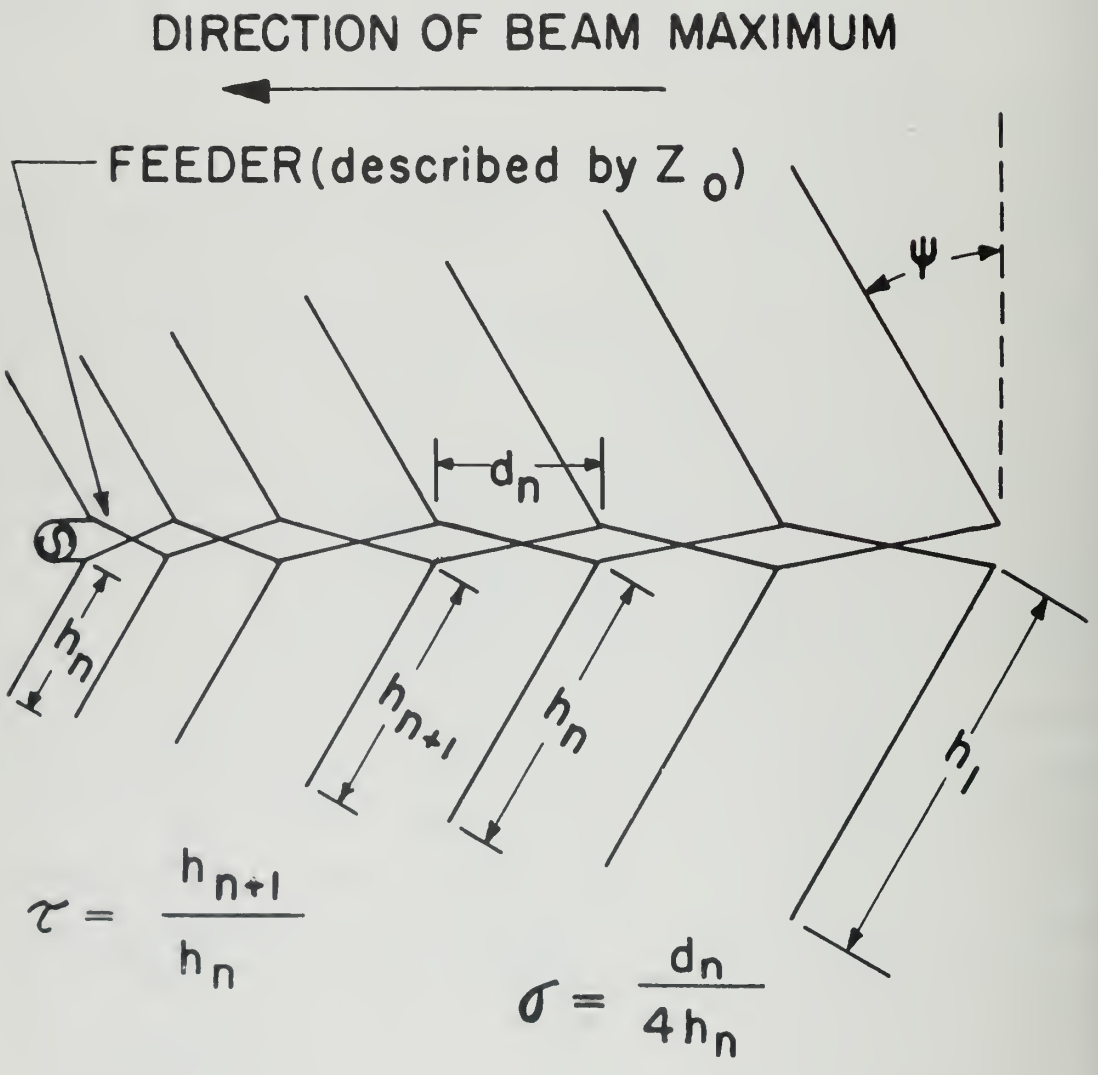

Figure 4. The Log-Periodic Resonant-V Array

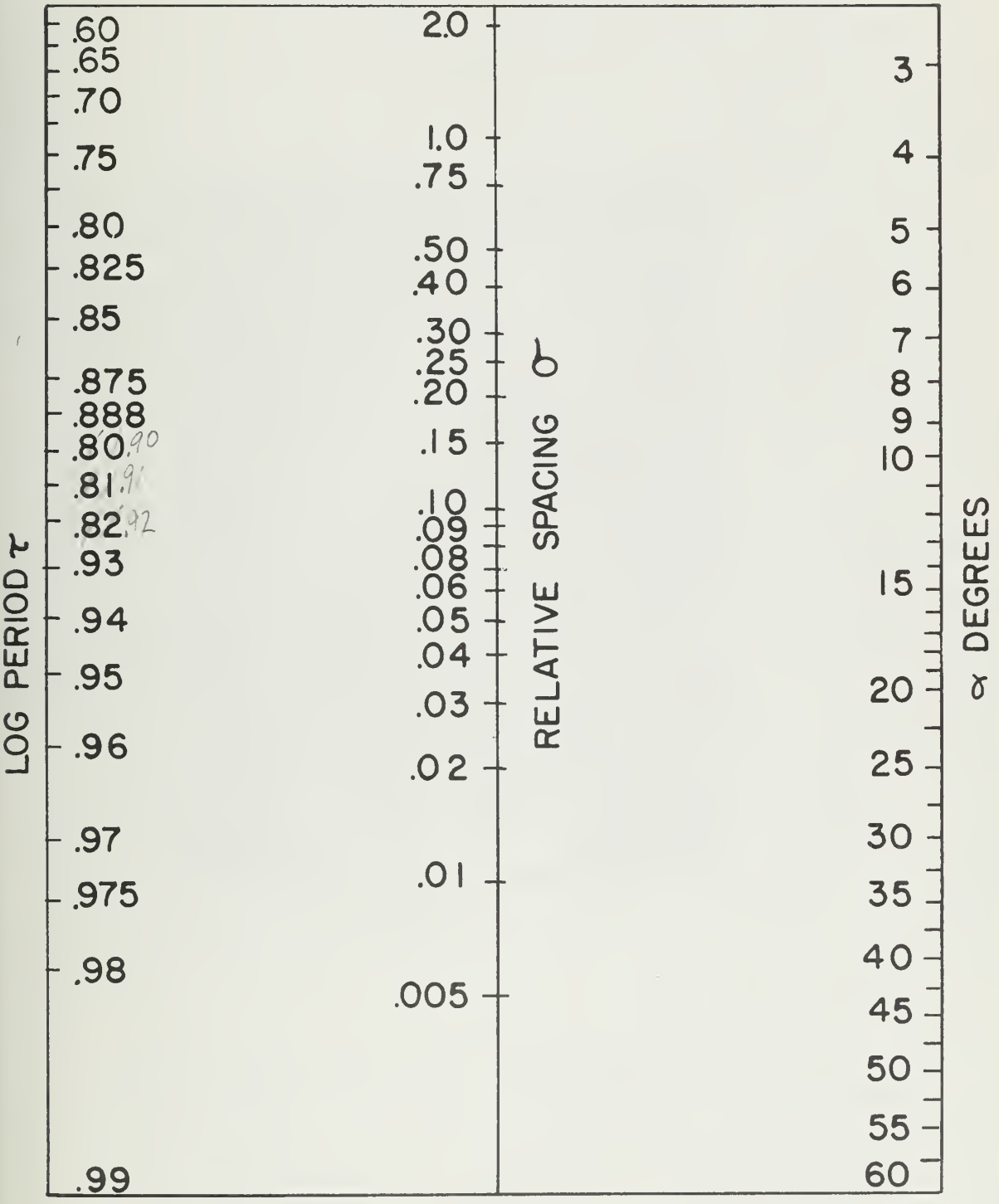

NOMOGRAPH OF

$$\sigma = \frac{1}{4}(1-\tilde{a})\cot\alpha$$

Figure 5

used for the elements. These antennas are fed with a coaxial cable in the same manner as the LP dipole arrays.[5] A microdot cable is threaded from rear to front through one of the hollow feeder conductors. The outer conductor of the cable is connected to one feeder conductor; the center conductor to the other. A frequency independent conversion from unbalanced to balanced line is made at the antenna feed point because of the manner in which the current diminishes along the structure due to radiation.

Because the feeder line usually carries negligible current past the active region, the termination of this line is relatively unimportant. For uniformity in the results and to provide mechanical support, a short circuit termination located a distance 1/2 h_1 behind the longest element was used in all the pattern models. The models tested and their parameters are listed in Table 1. A photograph of LPV - 8 is shown in Figure 6.

TABLE 1

Model No.	N*	τ	σ	ψ(Degrees)
LPV-1	20	0.95	0.0461	0,32.5,40,45,50
LPV-2	25	0.95	0.0694	0,45,50,55
LPV-3	25	0.95	0.0268	0,45,50,55,60,65
LPV-4	12	0.888	0.112	0,45,50
LPV-5	12	0.888	0.0444	45,55
LPV-6	12	0.888	0.025	45,55
LPV-7	14	0.91	0.0257	55
LPV-8	14	0.91	0.053	55
LPV-9	11	0.888	0.066	55

*Number of elements.

3.1.2 General Pattern Measurement Results and Interpretations

Radiation patterns were taken, starting at a frequency f_o near the low frequency bandlimit, at frequencies $\tau^{-p} f_o$ (p = integer or integer plus 1/2) until the high frequency bandlimit (or the upper frequency limit of the pattern range equipment) was encountered.

The patterns of the first models tested were good over most of the band. At some spots in the band, however, lobing of the patterns was observed and was often accompanied by a large cross-polarization component. It is to be expected that such behavior might occur at the "transition" frequencies

Figure 6. The Pattern Model of LPV-8.

between modes.

At the low frequency bandlimit the active region is located near a half-wavelength element at the rear of the structure. As frequency increases the active region moves toward the front of the antenna. Since the array is truncated on the front end also, a frequency will be reached at which there are no half-wave elements on the structure. If the ratio of largest to smallest element length exceeds 3, there will be a three-half-wavelength element at this frequency. There will be a band of frequencies, however, in which radiation will occur from the front elements, even though somewhat shorter than $\lambda/2$, as well as the $3\lambda/2$ elements toward the rear. When these two active regions radiate simultaneously from positions which are separated by distances of the order of the wavelength, the path difference between the two regions would be sufficient to cause lobing of the patterns.

It is likely, too, that the input impedance in the transition band would not be good, resulting in a smaller amount of radiation of the principlal polarization from the antenna. This would account for the higher relative level of the always present cross-polarized field. It was indeed found that most of the frequencies where lobing or other significant changes in pattern shape occurred could be included in the transition bands between various modes.

It was also found that the cross-polarized radiation could be reduced considerably by taking greater care in the construction. Figure 7 shows three types of construction that were used on one model (LPV-3) in order to compare performance. The construction shown in (c) was found to be superior to the others, displaying considerably lower cross-polarization and fewer pattern anomalies. A close-up photograph in Figure 8 further illustrates this method of bending the elements so that they all lie in the same plane.

3.1.3 Radiation Patterns and the Variation of ψ

The radiation pattern of the V elements depends upon the angle of the V. For each mode there is a different angle which produces maximum gain.[7]

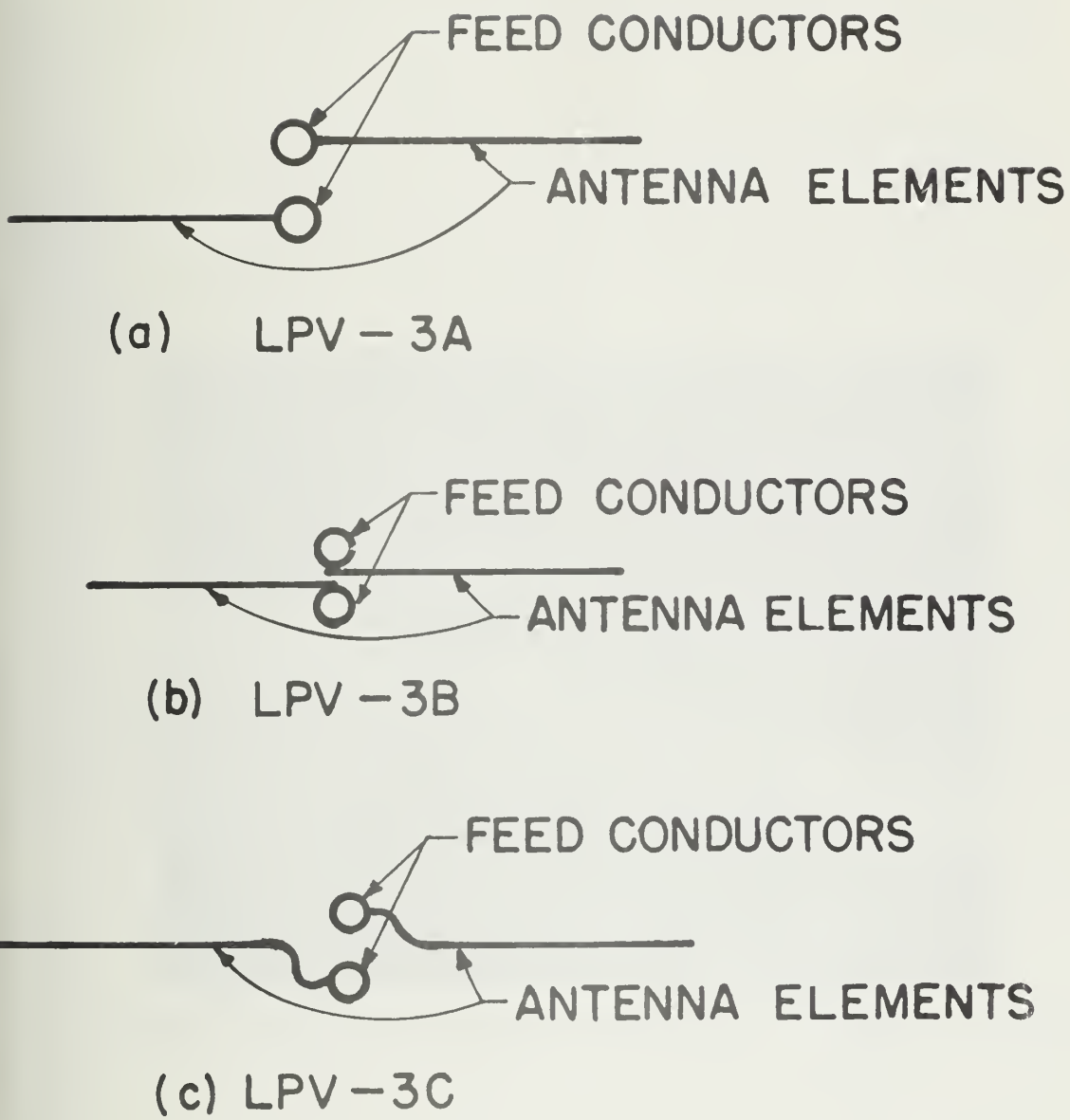

Figure 7. Methods of Feed for Three Versions of LPV-3 (In each case an end view of one pair of antenna elements is shown).

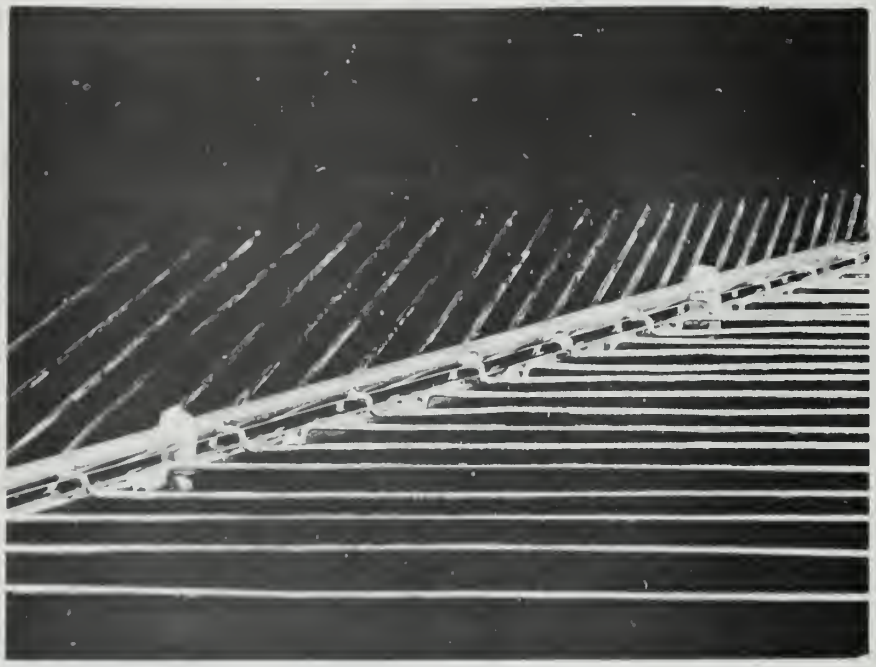

Figure 8. A Close-up View of LPV-3C Showing Method of Attaching Elements to Feed Line.

For the half-wavelength mode the angle Ψ for maximum gain is zero. However, the gain does not change much in this mode for other angles. For maximum directivity of the V in the $\frac{3\lambda}{2}$ mode, $\Psi \approx 32.5^{\circ}$; in the $\frac{5\lambda}{2}$ mode, $\Psi \approx 50^{\circ}$; in the $7\lambda/2$ mode, $\Psi \approx 52.5^{\circ}$.

An experimental study was made of the effect of changing Ψ in an LPV array. Radiation patterns for LPV-3A were measured for $\Psi = 45^{\circ}, 50^{\circ}, 55^{\circ}, 60^{\circ}, 65^{\circ}$. The principal change in the radiation pattern caused by changing Ψ was a change in sidelobe level when operating the LPV array in the higher order modes. The sidelobe levels decrease as Ψ is increased. Data concerning the side-lobe of LPV-3A are shown in Figure 9.

3.1.4 Radiation Patterns and Directivity Data

The directivity in decibels over an isotropic radiator can be computed approximately from the formula

$$D = 10 \log_{10} \frac{41250}{(BW_E)(BW_H)} \qquad (2)$$

where BW_E and BW_H are the half-power beamwidths in degrees in the E and H planes, respectively.[8] This formula ignores the effect of sidelobes on the directivity but is accurate to a fraction of a decibel when the sidelobes are more than 10 db down from the maximum.

Plots of directivity computed from Equation 2 are shown in Figure 10 for LPV-3A for several values of Ψ. The increase in directivity with higher mode operation is clearly seen in these data. The directivity has been averaged over each mode for the various Ψ angles and the average directivity is plotted in Figure 11.

Operation of the LPV arrays in the $\lambda/2$ mode is similar to that of the LP dipole arrays. The only significant difference is a broadening of the beamwidths due to the reduced directivity of the half-wave dipole when bent to form a V. Typical E and H-plane patterns of LPV-3C in the $\lambda/2$ mode are shown in Figure 12 and for LPV-2 in Figure 13. Principal polarization patterns are shown with dashed lines; cross polarization with solid lines.

As the frequency increases so that the LPV array is operated in the higher order modes the principal changes in the pattern are narrower beamwidths and the appearance of sidelobes. Typical patterns of LPV-3C in the higher order modes are shown in Figures 14-16.

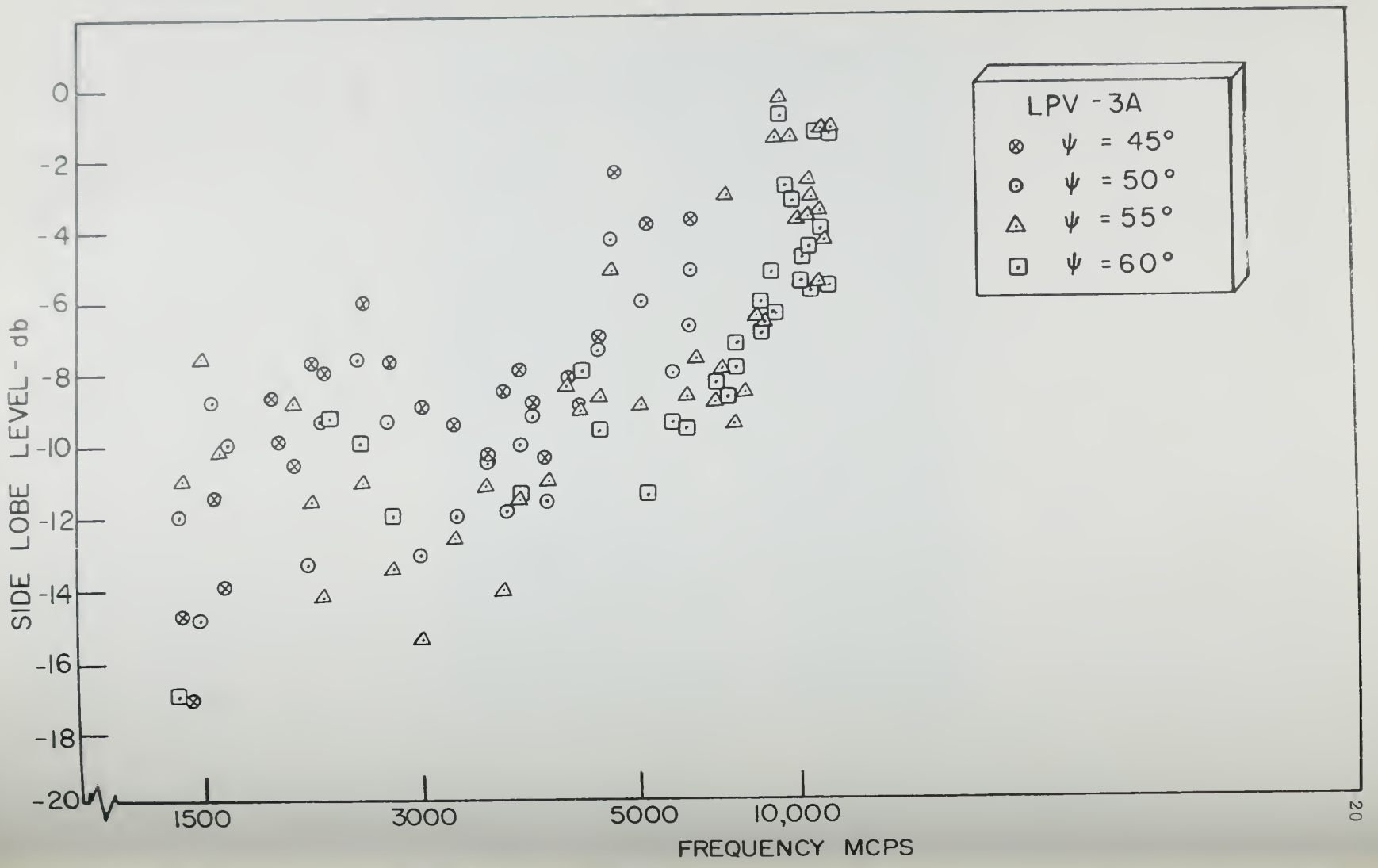
LPV - 3A
ψ = 45°
ψ = 50°
ψ = 55°
ψ = 60°
SIDE LOBE LEVEL - db
0
-2
-4
-6
-8
-10
-12
-14
-16
-18
-20
1500
3000
5000
10,000
FREQUENCY MCPS

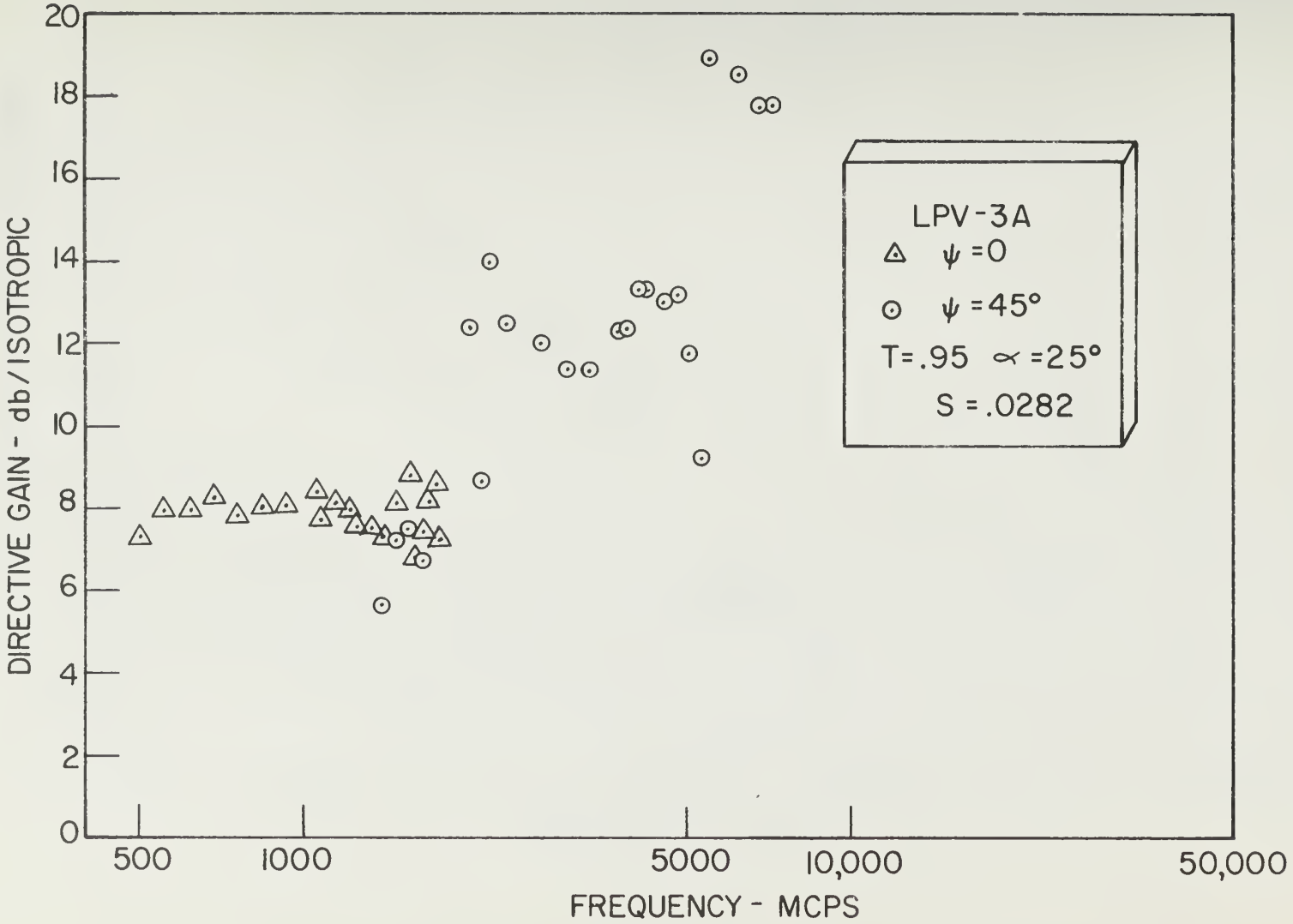
DIRECTIVE GAIN - db/ISOTROPIC
20
18
16
14
12
10
8
6
4
2
0
500
1000
5000
10,000
50,000
FREQUENCY - MCPS
LPV-3A
ψ =0
ψ =45°
T=.95 ∝ =25°
S =.0282

Figure 10a

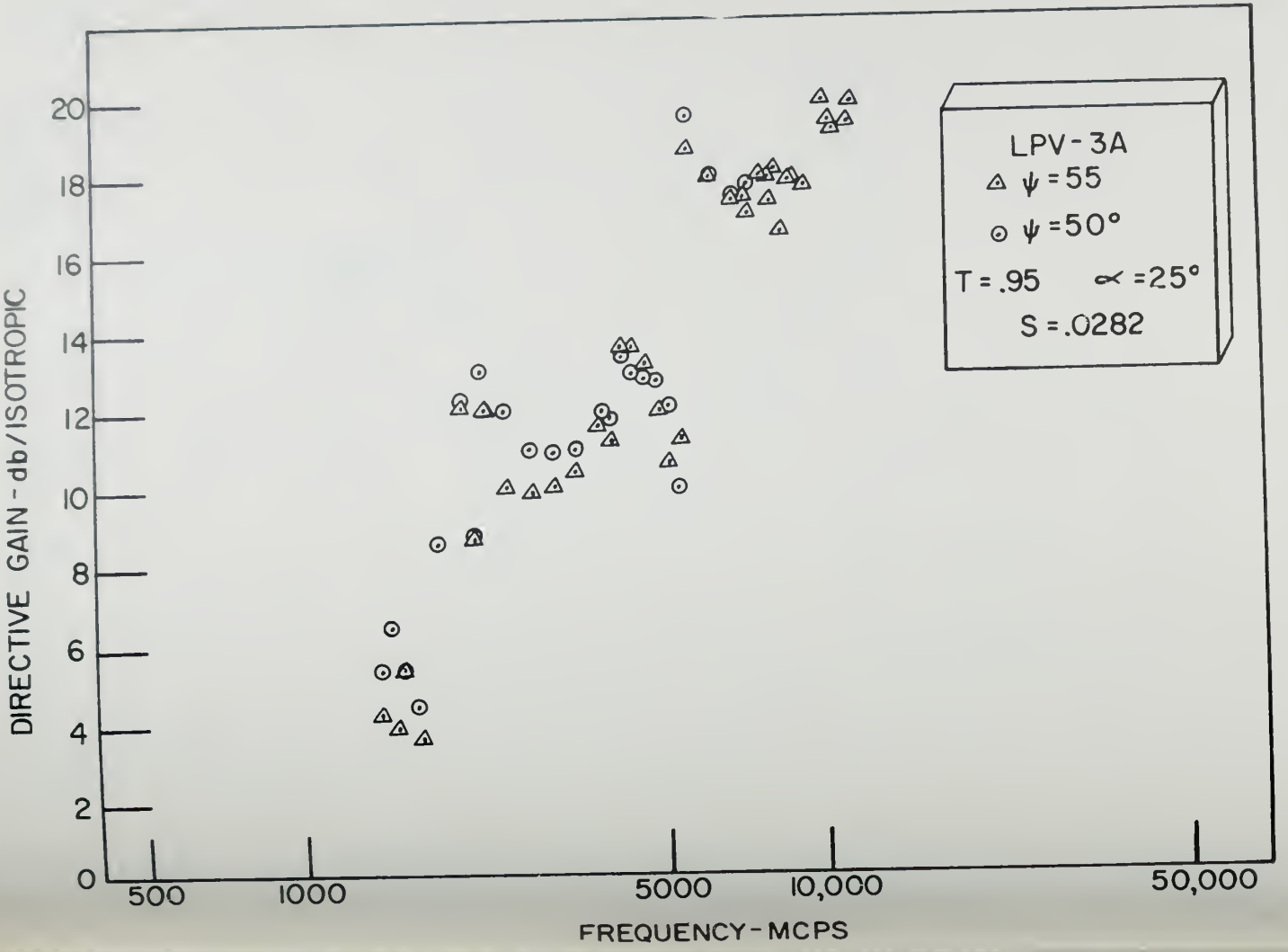
LPV-3A
△ ψ=55
⊙ ψ=50°
T=.95 ∝=25°
S=.0282
DIRECTIVE GAIN - db/ISOTROPIC
FREQUENCY - MCPS
0
2
4
6
8
10
12
14
16
18
20
500
1000
5000
10,000
50,000

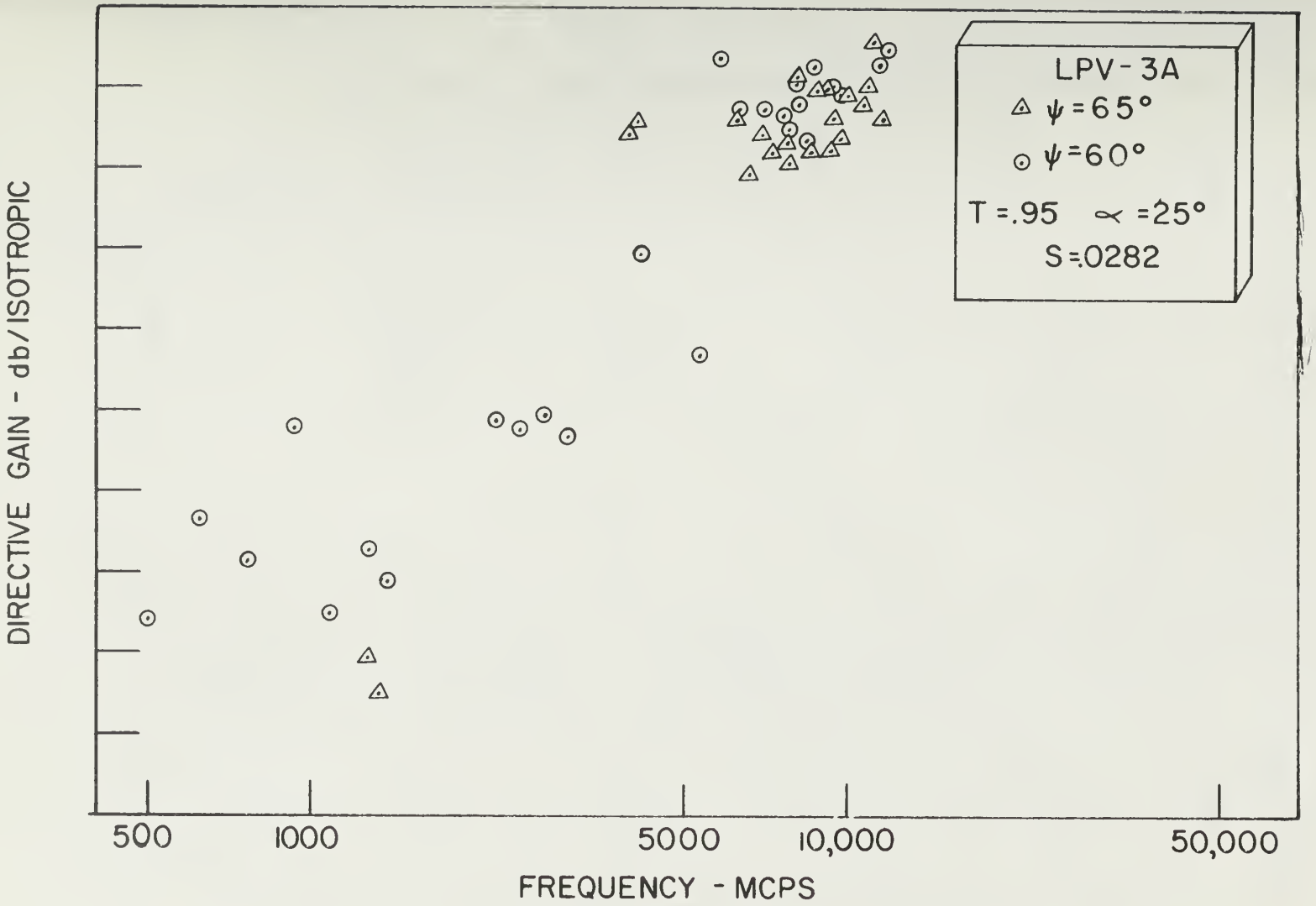
LPV - 3A
△ ψ = 65°
⊙ ψ = 60°
T = .95 ∝ = 25°
S = .0282
DIRECTIVE GAIN - db/ISOTROPIC
500
1000
5000
10,000
50,000
FREQUENCY - MCPS

Figure 10c

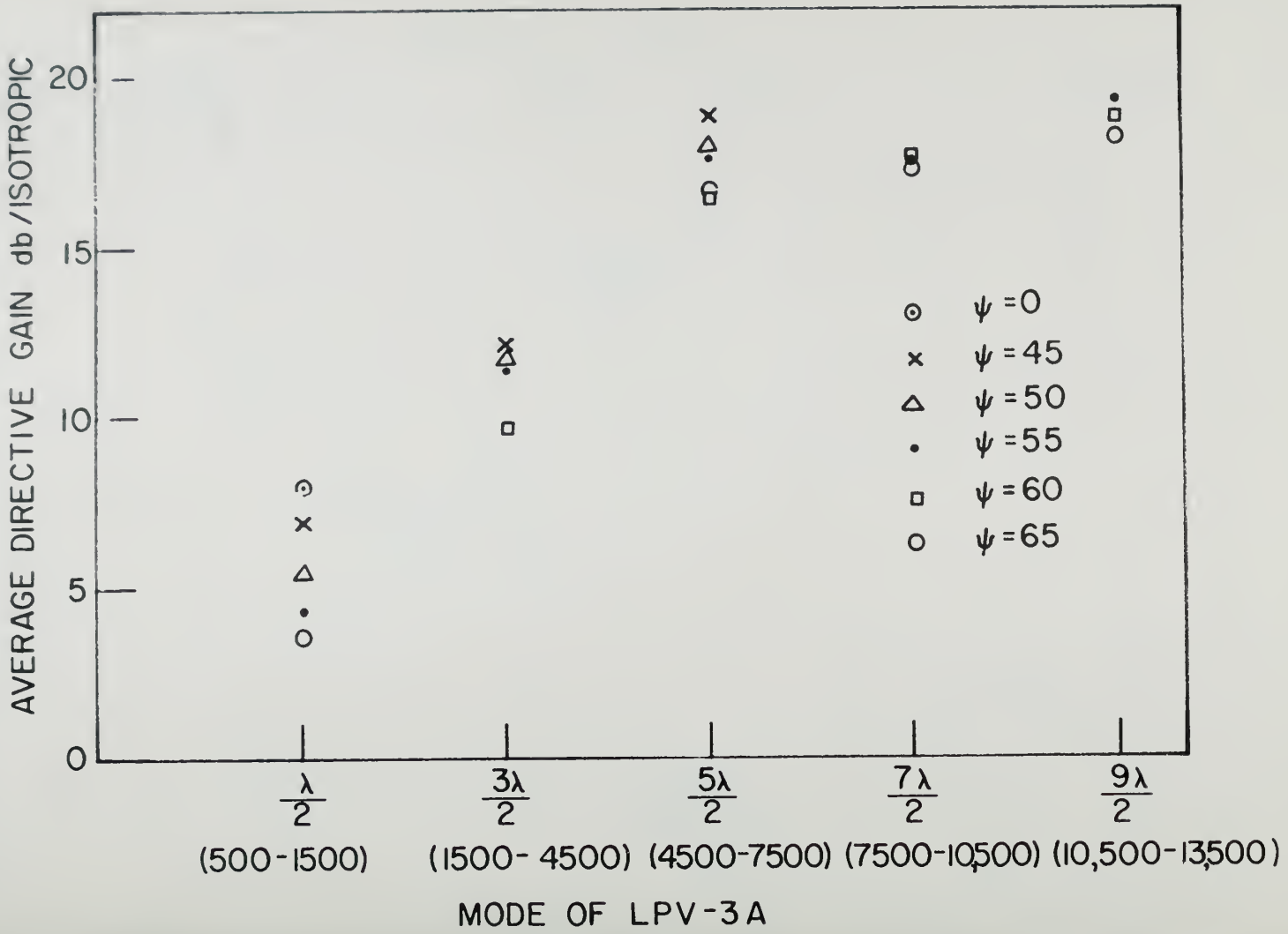
AVERAGE DIRECTIVE GAIN db/ISOTROPIC
20
15
10
5
0
ψ = 0
ψ = 45
ψ = 50
ψ = 55
ψ = 60
ψ = 65
λ/2
3λ/2
5λ/2
7λ/2
9λ/2
(500-1500)
(1500-4500)
(4500-7500)
(7500-10,500)
(10,500-13,500)
MODE OF LPV-3A

Figure 11

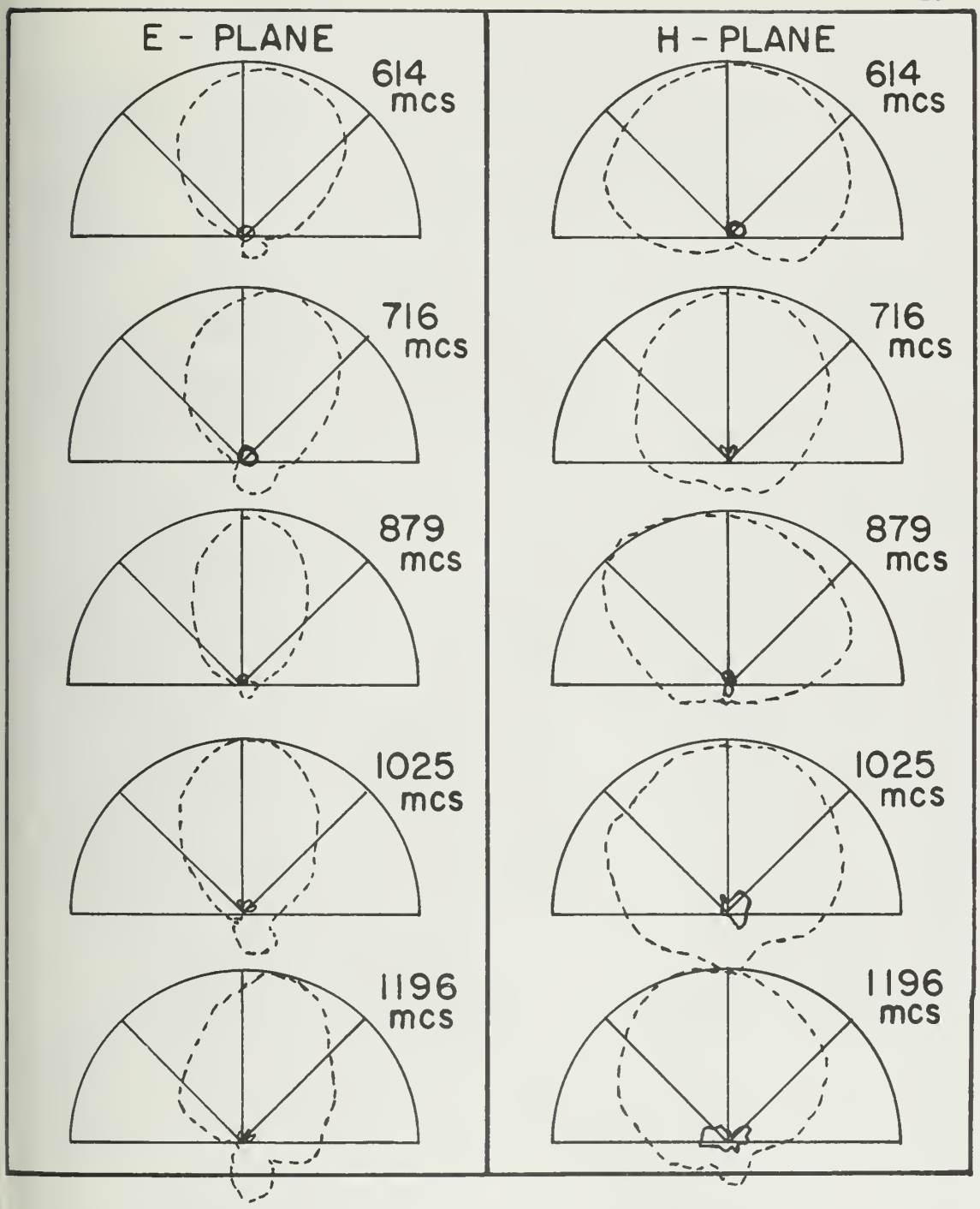

Figure 12. Radiation patterns of LPV-3c in $\lambda/2$ mode, $\psi = 60^{o}$

- - - - - Principal polarization

_____ Cross polarization

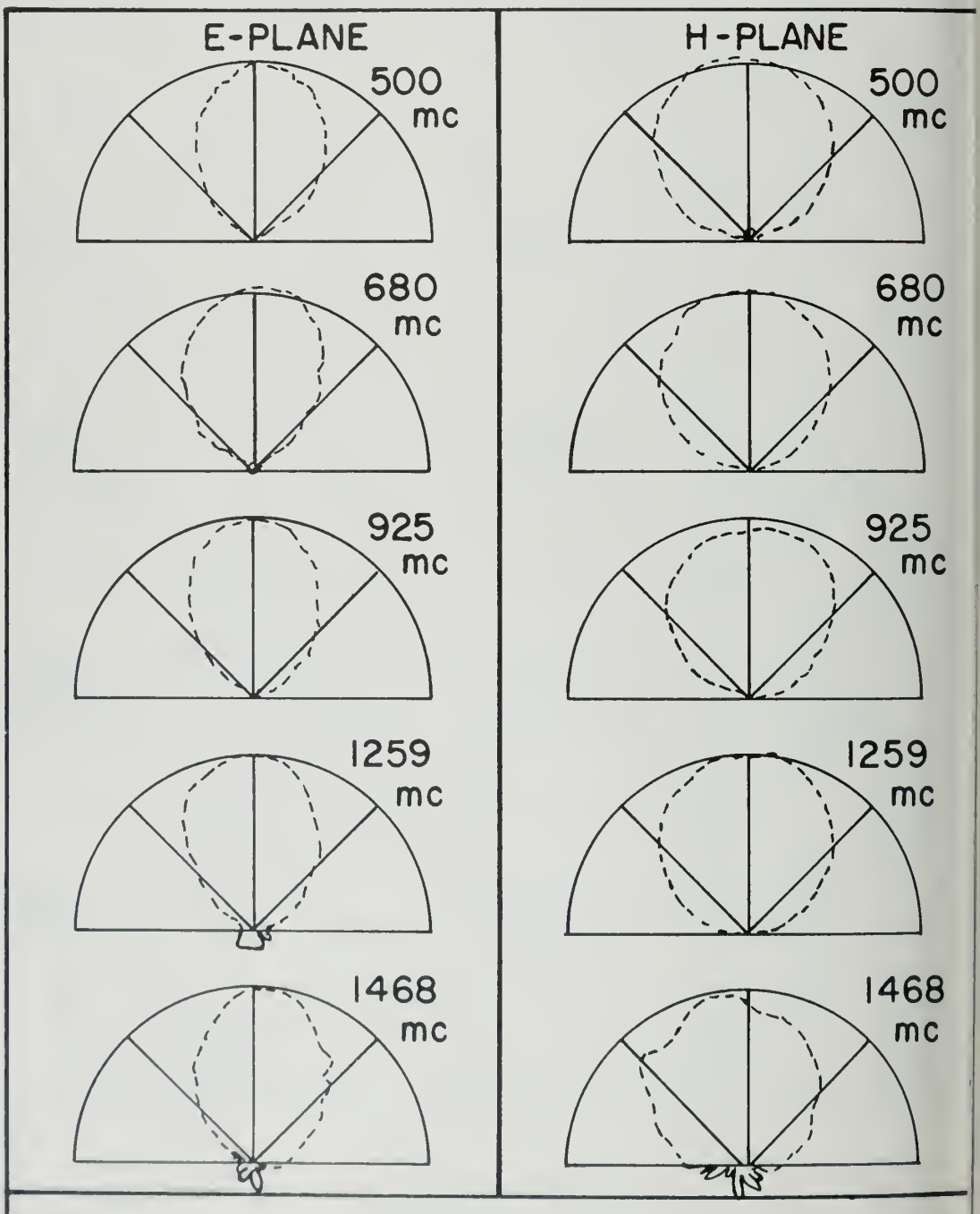

Figure 13. Radiation patterns of LPV-2 in $\lambda/2$ mode, $\psi = 50^{\circ}$
(Cross polarization not recorded)

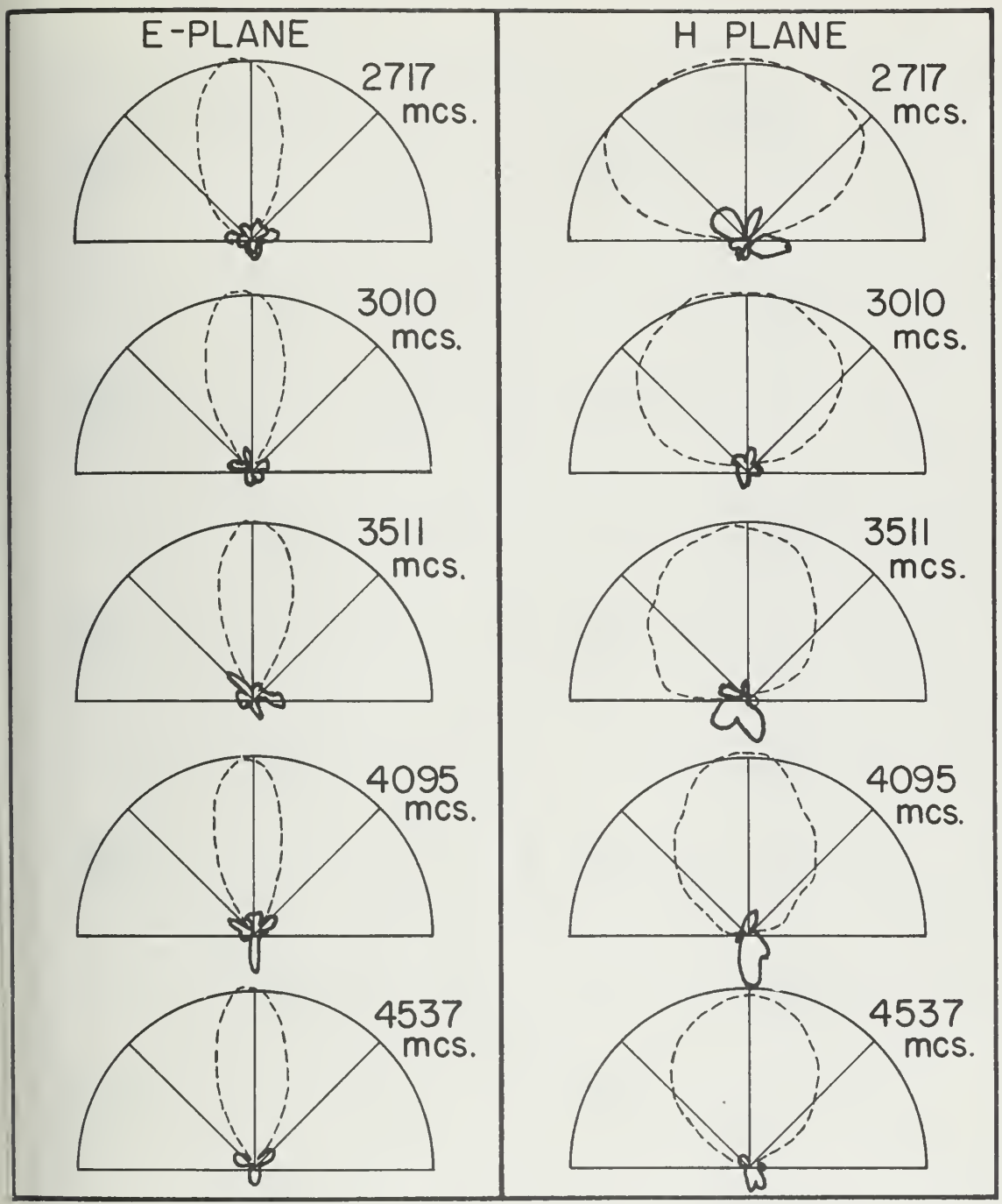

Figure 14. Radiation patterns of LPV-3c in $3\lambda/2$ mode

- - - - - principal polarization

_____ cross polarization

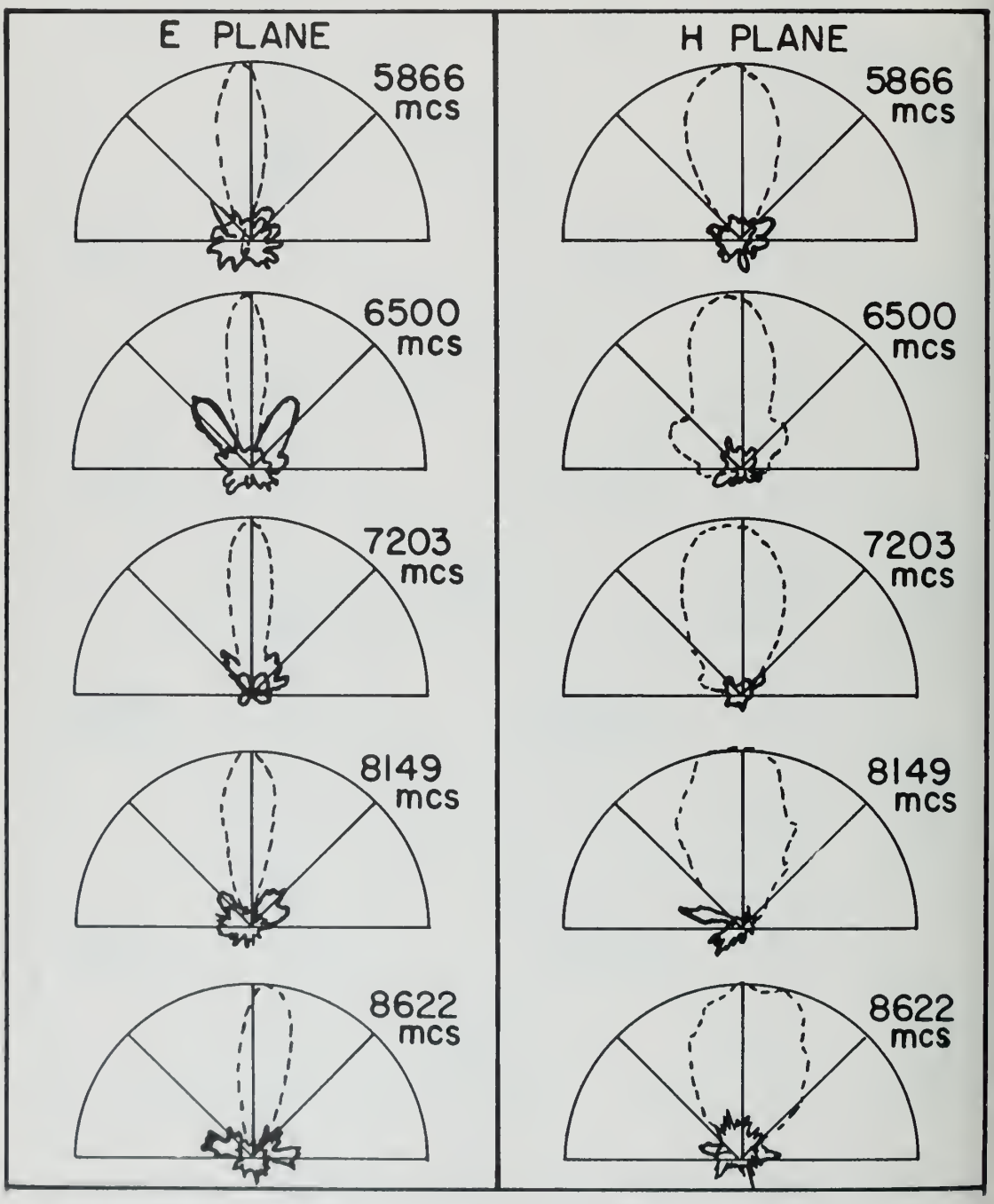

Figure 15. Radiation patterns of LPV-3c in 5λ/2 mode

- - - - - principal polarization

——————— cross polarization

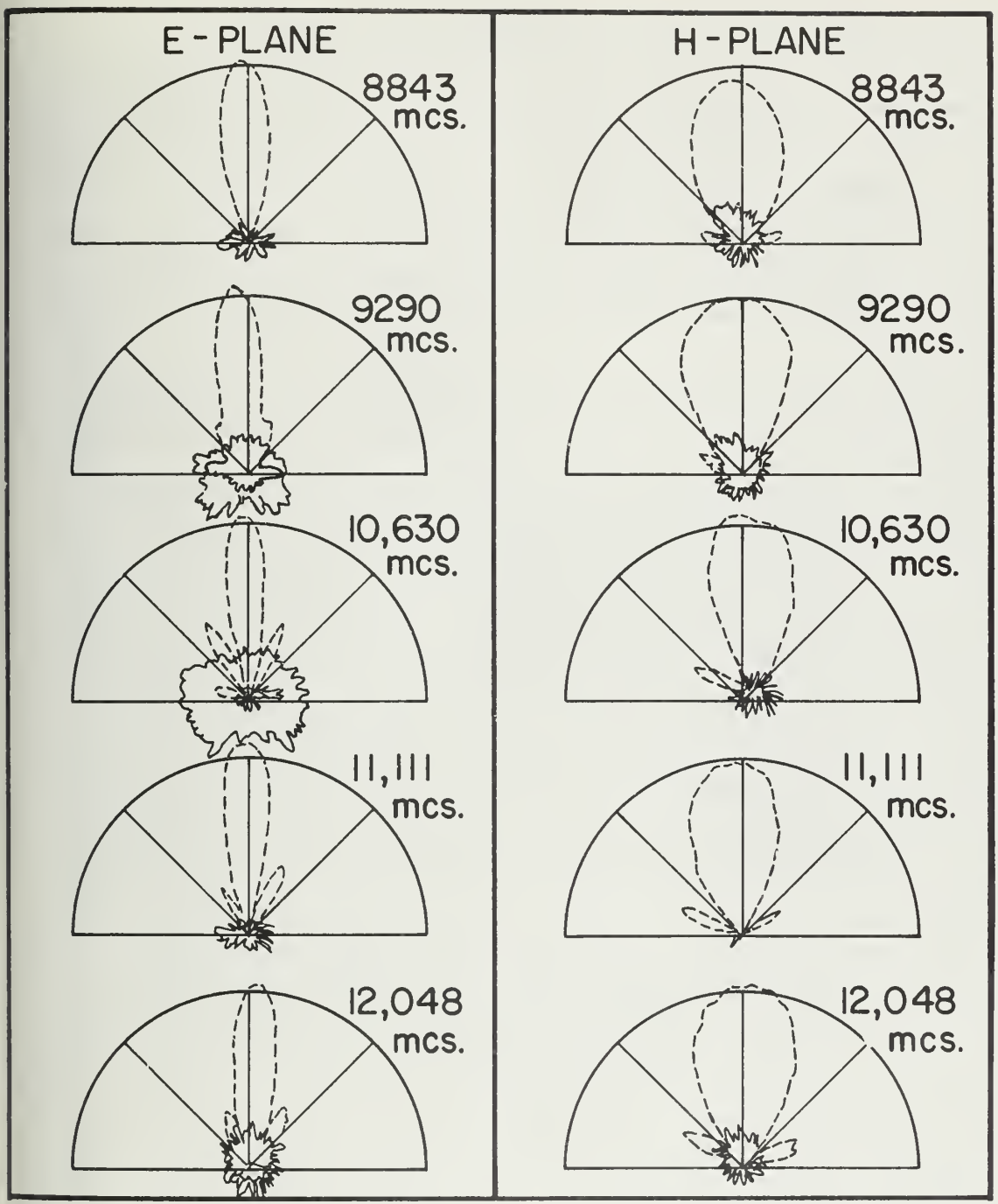

Figure 16. Radiation patterns of LPV-3c in $7\lambda/2$ mode

- - - - - Principal polarization

_____ Cross polarization

3.1.5 Minimum Array Length and Maximum Element Spacing

Beyond the fact that there must be a half-wavelength element on the antenna at the lowest frequency, the dipole and resonant-V arrays have a minimum length at the lowest frequency. If the total array length does not exceed the length of the active region of an infinite structure with the same parameters at the same frequency, then the array factor will differ from that of the infinite structure. This is generally characterized by a decrease in front to back ratio as the frequency decreases below this critical point.

Since the length of the active region depends upon α particularly, the minimum length required to reach a certain lower frequency likewise is a function of α. The limited amount of data concerning this dependence as determined from the pattern measurements is plotted in Figure 17. The maximum wavelength for satisfactory operation was estimated by comparing front to back ratio at various frequencies on the several pattern models. The length of the array L has been normalized with respect to the maximum wavelength in each case and these normalized lengths are plotted as a function of α in Figure 17. There is some scattering of the data due to a secondary dependence upon τ, three different values being used in the data of Figure 17. The general trend as a function of α is nevertheless apparent and the expected longer required length for small values of α is illustrated.

Satisfactory operation in the higher order modes is primarily contingent upon the spacing between elements, although τ also seems to have a secondary effect. The highest frequency of operation with well-formed beams is shown in Table 2 for each of the LPV pattern models. The mode number n, designating the number of half-wavelengths of the mode wherein the maximum frequency is found, is also indicated along with n times the spacing parameter σ. This latter product ($n\sigma$) gives approximately the element spacing in wavelengths at the maximum frequency. Note that in all cases this spacing is less than three-eighth wavelength and in several cases is approximately equal to one-quarter wavelength.

The foregoing considerations outline limitations on design. They do not necessarily provide for optimum performance accross the entire band. Generally speaking, operation is improved by increasing τ and decreasing σ so that the best performance is obtained from the antennas having a larger

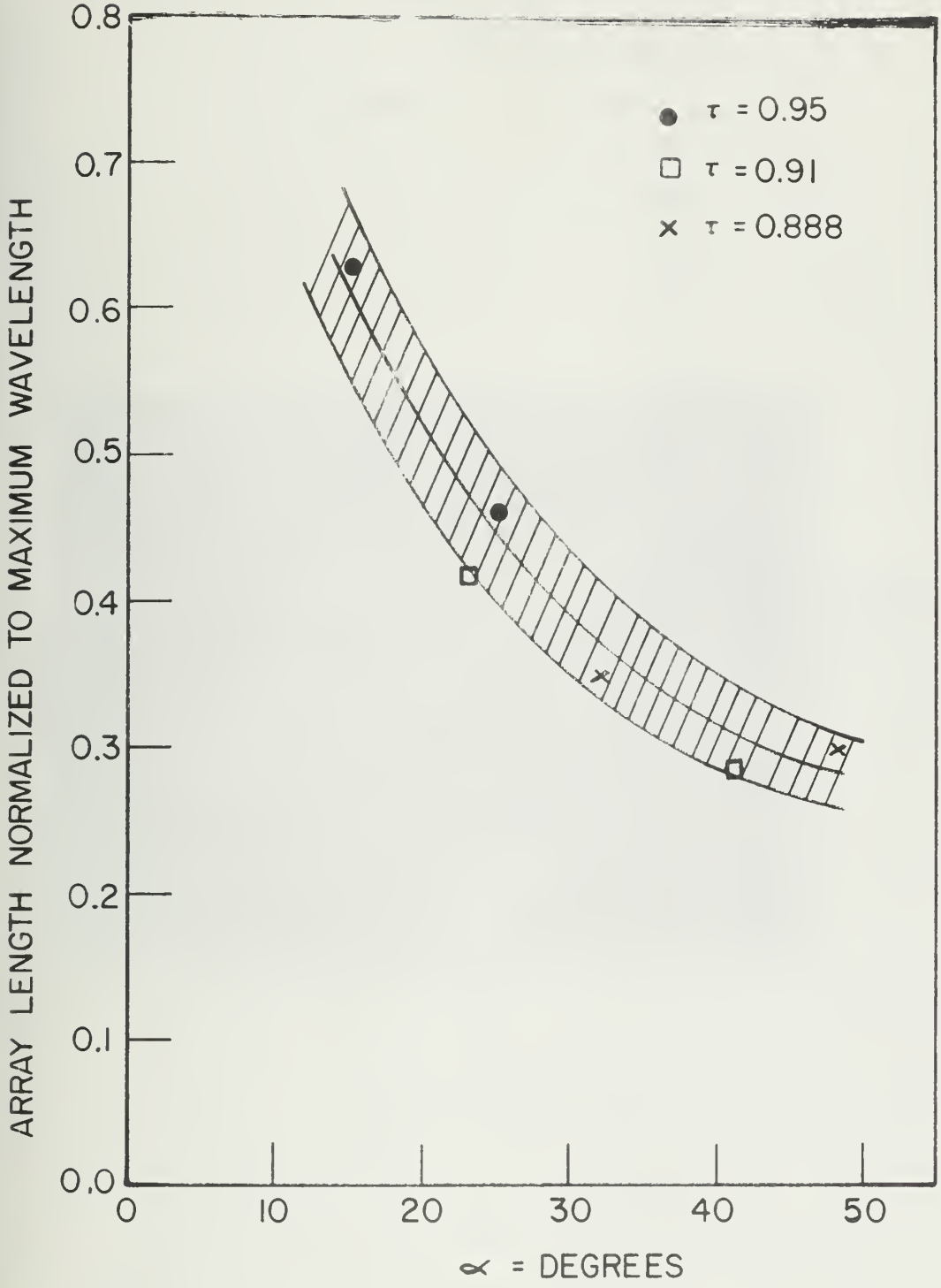

Figure 17. Minimum Length as a Function of Angle α for LPV Arrays

number of elements. Of the antennas tested in the pattern investigation LPV-3 maintained the best performance over the widest frequency band.

TABLE 2

	f_{max} in mcs	Mode No. n	$n\sigma$
LPV-1	7000	5	0.23
LPV-2	5500	5	0.34
LPV-3	12000	9	0.25
LPV-4	2500	3	0.34
LPV-5	9000	7	0.31
LPV-6	11000	9	0.23
LPV-7	12000	9	0.23
LPV-8	9000	7	0.37
LPV-9	6000	5	0.33

3.2 Impedance Measurements

The pattern models of the LPV antennas could not be used for the measure of the input impedance for two reasons. First, the construction tolerances could not be held to as small a fraction of the wavelength as was deemed necessary and second, the losses and inhomogeneities of the Microdot feeder coax would invalidate the measured value of impedance. For these reasons a separate program was undertaken to measure the input impedance of the LPV arrays for as many values of the parameters as was practical, in order to compile data which could be used as a basis for the design of LPV antennas. In addition, correlation between the pattern and impedance data was sought.

3.2.1 Construction of the Impedance Models

Since the radiation properties of the LPV-3A were the best of all pattern models up to the time at which the impedance program was initiated, it was decided to use the LPV-3A design for the impedance model. (In LPV-3A the elements and their respective conductor are coplanar). ILPV-3A is shown in Figure 18. The impedance model is scaled up from LPV-3A by a factor of 2.8:1; the 0.410 inch diameter of the feeder permits the use of RG-115A, a low loss, teflon dielectric coaxial cable for the feed coax. Preliminary measurements showed that the small loss in the length of

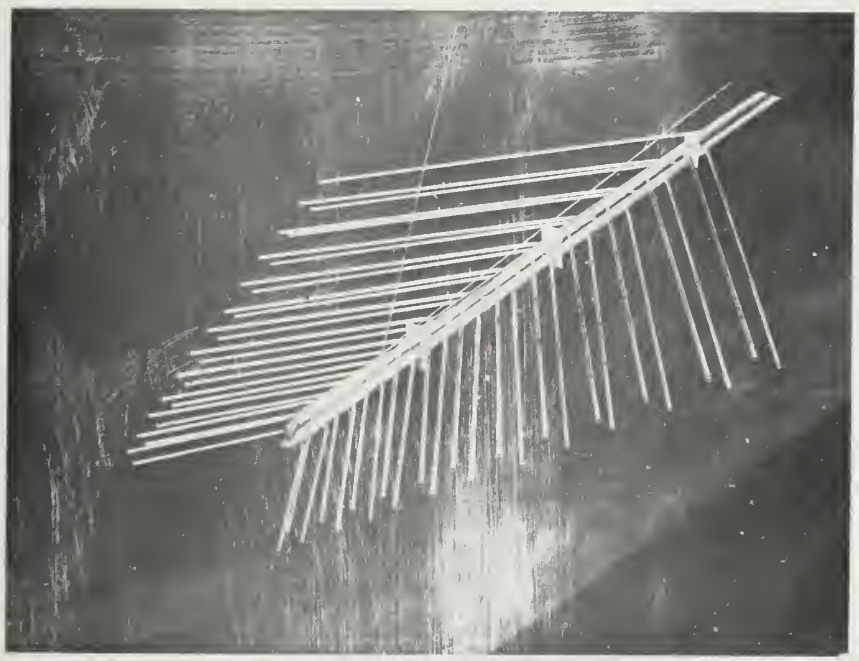

Figure 18. Model ILPV-3 Used for Impedance Measurements.

cable could be neglected in the measurement of standing wave ratios of 4:1 or less. The feeder and elements were made of coin silver tubing. The half length, h, of the largest element is 16.8 inches and the smallest, 4.9 inches. The element diameter was held constant at 0.140 inches, which means that the h/a ratio varies from 80 to 240. The length of the section of feeder along which the elements are attached is 25.5 inches. An additional 8.4 inches of feeder beyond the largest element is terminated in a short circuit to eliminate the possibility of end effect current interfering with the measuring equipment. The value of τ is 0.95 and σ is 0.0266. ψ angles of $40^{\circ}, 45^{\circ}, 50^{\circ}$, and 55° were obtained by bending the elements which are silver-soldered onto the feeders. Built into this model was a provision for easily adjusting this characteristic impedance of the feeder, Z_o, to values of 75,100,125, or 150 ohms. The accuracy was least for the 150 ohm value because of the error incurred due to the larger gap at the feed point. It can be seen that ILPV-3A, with its superior feed coax, eliminates the objections to the use of the pattern models for impedance measurements.

3.2.2 Description of the Measurements and the Measuring Equipment

The input impedance was measured as a function of frequency every half-period according to the formula

$$f_{n/2} = f_o \tau^{-n/2}, \quad n = 0, 1, 2, \text{---}.$$

The frequencies covered were from $f_o = 161.2$ mcs to $f_{63} = 3882$ mcs. In order to cover this wide frequency range (24:1) two different measuring devices were used. Below 640 mcs the impedance measuring device was the PRD type 219 standing wave indicator which measures the reflection coefficient by means of a crystal-and-probe assembly which is rotatable in a calibrated drum, corresponding to the movement of the conventional probe in a slotted line. Above 640 mcs, a Hewlett-Packard model 805-A slotted line was used to measure the standing wave ratio and position of voltage minimum. Several different oscillators were used to cover the frequency range. A heterodyne frequency meter assured repetition of the various frequencies. A picture of the impedance set up is shown in Figure 19. Note that the antenna and all equipment are mounted on a bench equipped with casters. During the performance of any set of measurements, the whole set up is rolled to a

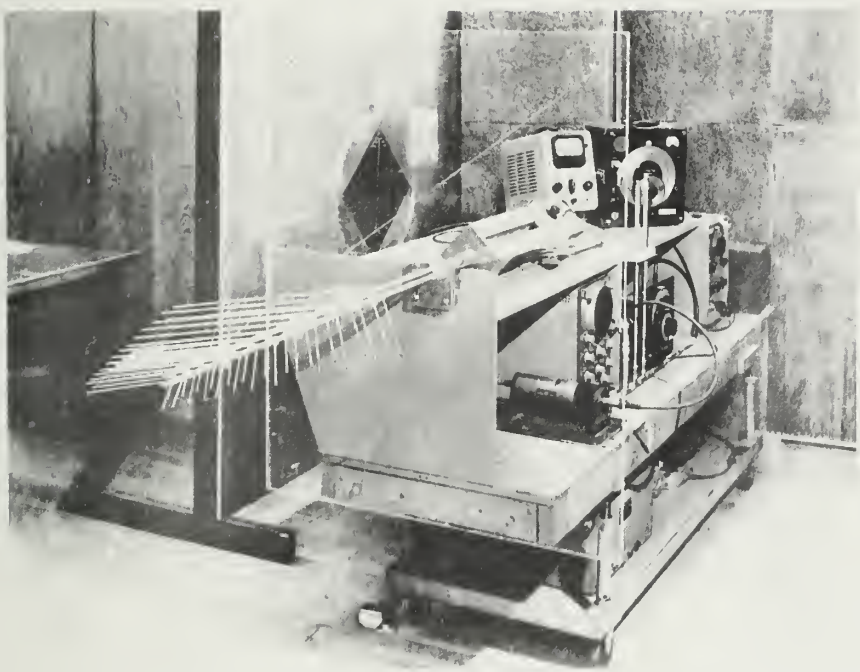

Figure 19. Impedance Measuring Set-up

specially constructed window in the wall of the antenna laboratory, which is on the second floor of the building. Thus the measurements are performed on the inside while the antenna is looking into an uncluttered environment. The impedance measuring set up is shown schematically in Figure 20. It is essential to use a low pass filter as indicated in the diagram, because satisfactory operation of the PRD Standing Wave Indicator as well as the slotted line requires a strictly monochromatic signal. In each measurement the impedance is referred to the input terminals at the front of the antenna. The reference used in the null shift method was determined by a measurement of the short circuited feedpoint as a function of frequency through the 37 inches of RG-11SA coaxial cable.

3.2.3 General Results of the Measurements of Impedance on LP Structures

The results of the impedance measurements can be analyzed by comparing them with the impedance characteristics of the LP dipole array. In the LPDA the impedance is an almost periodic function of the logarithm frequency, the period being $\log \tau$. The slight deviation from periodicity is due to the necessary truncation at the front of the antenna. This front truncation means that the section of feeder from the feed point out to the "active" region is not scaled exactly with frequency, resulting in an impedance transformation which is a function of frequency, causing a translation of the impedance locus. The input impedance of the LPDA is predominately real and is centered at 55 to 100 ohms. The SWR measured in practice varies from 1.3:1 to 2:1 when using the center resistance value R_o as a reference for the SWR. R_o is determined by drawing a circle which encloses the locus of the measured impedances on a Smith chart. The circle is centered on the resistance axis, and the value of R_o is given by

$$R_o = \sqrt{R_{max} R_{min}} \tag{3}$$

where R_{max} and R_{min} are respectively the maximum resistance and the minimum resistance given by the intersection of the circle with the resistance axis. The maximum standing wave ratio with respect to R_o is given by

$$VSWR = \sqrt{\frac{R_{max}}{R_{min}}} \tag{4}$$

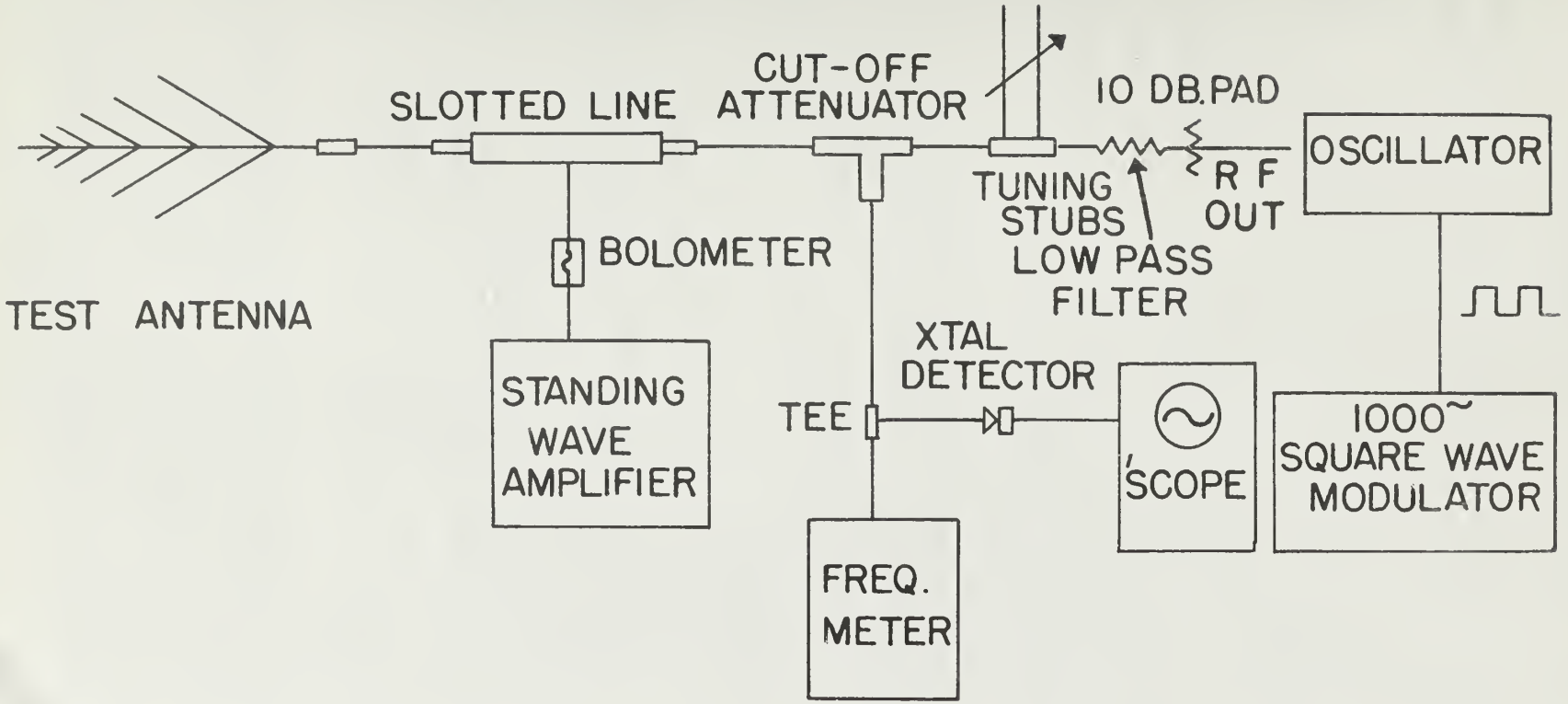

Figure 20. Block Diagram of Impedance Measuring Set-Up

3.2.4 Input Impedance: Single Mode Operation

Considering any one mode of operation, one finds that the impedance characteristic of the LPVA is comparable with that of the LPDA. The impedance within a given mode is predominately real, clustered about some R_o. Figure 21(b) shows the maximum SWR which may be expected in any one mode, referred to the R_o of that mode. The maximum SWR varies from 1.4 to 1.8 and is not strongly dependent on the feeder characteristic impedance Z_o. Figure 21(a) shows a plot of the center resistance value R_o for the various LPV modes vs. the characteristic impedance of the feeder. It shows that the center value R_o for each mode increases with Z_o in a non-linear fashion. This behavior is also demonstrated in the LPDA. Thus control of the impedance level can be accomplished by controlling the feeder characteristic impedance. In Figure 21 the Ψ angle was held at 50^o; similar variations were obtained with Ψ angles from 40^o to 55^o.

3.2.5 Input Impedance: Multi-Mode Operation

Figure 22 illustrates the impedance variation over the whole range of frequencies. Since any attempt to draw a line connecting all the measured points would lead to a complicated graph, the impedance locus is plotted as follows: All points which lie in a given mode are enclosed by a circle which represents the maximum SWR of each mode. In Figure 22 the four modes shown are the $\lambda/2$, $3\lambda/2$, $5\lambda/2$, and $7\lambda/2$. As the transition range is entered, that is, for frequencies in which the operation changes from one mode to another, the impedance locus departs from one of the mode circles and rapidly swings out and around the Smith chart, until the next mode circle is entered. The frequencies noted on the chart are the entrance and exit frequencies for each mode, in addition to a few frequencies in the transition region. For this Figure Ψ is 50^o and Z_o is 100 ohms. Their values were chosen because they are representative of the data which have been recorded to date.

3.2.5.1 Determination of the Weighted Mean Resistance Level R_{WM}

If it is desired to operate over the several modes, a compromise must be made to determine a fixed input impedance level. This level may be fixed by external considerations such as the desirability of using certain coaxial feed lines or the necessity of matching source or receiver impedance.

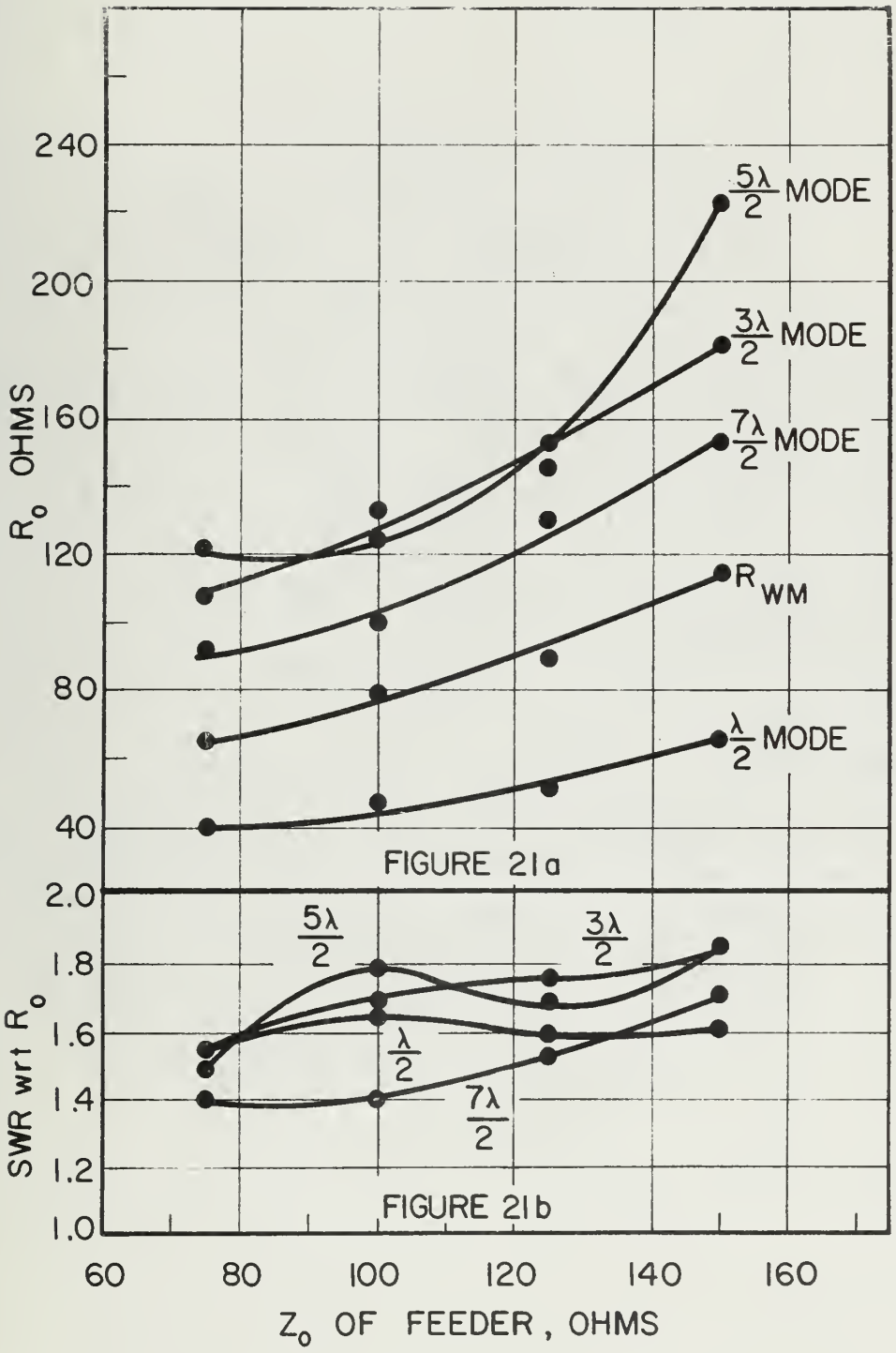

Figure 21. Resistance Level R_o and SWR with Respect to R_o for Each Mode vs. Characteristic Impedance of Feeder for $\psi = 50^o$.

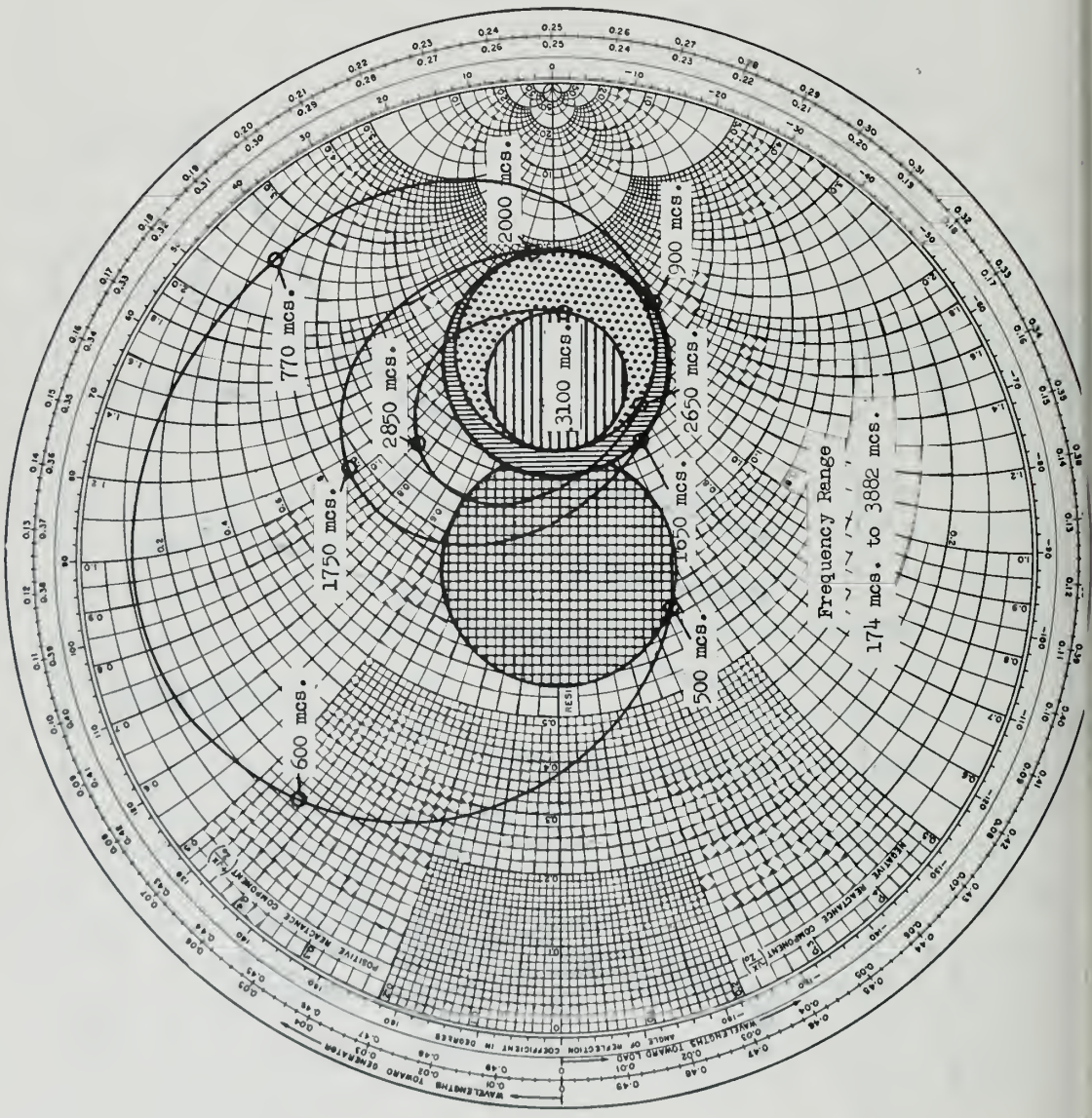

Figure 22. Impedance Plot

However, for the purpose of the display of data herein, a resistance which is called the weighted mean resistance level, R_{WM}, has been selected. R_{WM} is determined by the collection of measured points in the $\lambda/2$ and $3\lambda/2$ mode from this requirement: It is desired that the maximum standing wave ratio with respect to R_{WM} for both the $\lambda/2$ and $3\lambda/2$ modes be equal. Thus the expressions for standing wave ratio in terms of the maximum and minimum resistance values as read from the two mode circles (from a plot similar to Figure 22) are equated. Accordingly

$$SWR_{WM\ 1,2} = \frac{1 + |\rho_{1,2}|}{1 - |\rho_{1,2}|} \tag{5}$$

where $|\rho_{1,2}|$ is the maximum magnitude of the reflection coefficient in the $\frac{\lambda}{2}$ mode with respect to R_{WM} as the center. The maximum magnitude of $\rho_{1,2}$ is given by the hyperbolic distance between R_{WM} and the minimum resistance level encountered in the $\frac{\lambda}{2}$ mode, the minimum level is $R_{o\ 1,2}/SWR_{1,2}$. (The fraction subscripts indicate the mode). Therefore,

$$|\rho_{1,2}| = \left| \frac{R_{o\ 1,2}/SWR_{1,2} - R_{WM}}{R_{o\ 1,2}/SWR_{1,2} + R_{WM}} \right| \tag{6}$$

The maximum magnitude of $\rho_{3,2}$ is given by the hyperbolic distance between R_{WM} and the maximum resistance level encountered in the 3,2 mode; the maximum level is $R_{o\ 3,2}\ SWR_{3,2}$. Thus

$$|\rho_{3,2}| = \left| \frac{R_{o\ 3,2}\ SWR_{3,2} - R_{WM}}{R_{o\ 3,2}\ SWR_{3,2} + R_{WM}} \right| \tag{7}$$

Hence

$$SWR_{WM\ 3,2} = \frac{1 + |\rho_{3,2}|}{1 - |\rho_{3,2}|} \tag{8}$$

The reason for choosing the minimum level in the 1,2 mode and the maximum level in the 3,2 mode is that in every case measured so far

$$R_{o\ 1,2} < R_{WM} < R_{o\ 3,2} \tag{9}$$

Equating (5) and (8) using (6) and (7) with the condition (9) we can solve for R_{WM} and find that

$$R_{WM} = \sqrt{R_{o\ 1/2}\ R_{o\ 3/2}\ \frac{SWR_{3/2}}{SWR_{1/2}}} \qquad (10)$$

Thus R_{WM} differs from the geometric mean $\sqrt{R_{o\ 1/2}\ R_{o\ 3/2}}$ by a weighting factor which takes into account the relative difference which may exist between the maximum standing wave ratios which occur in each mode.

3.2.5.2 R_{WM} as a Function of LPVA Parameters

Figure 23 shows a graph of R_{WM} vs Z_o of the feeder for several values of ψ. Note the nearly linear relationship between R_{WM} and Z_o, and also note the insensitivity to ψ in the region where Z_o = 100 ohms. Using the data of Figure 23 a graph can now be plotted which shows how the standing wave ratio with respect to R_{WM} varies over the band. See Figure 24. A Z_o of 100 Ω and a ψ of 50^o were again chosen as representative. The transition regions are marked by an increase in the standing wave ratio and are clearly evident in Figure 24. The standing wave ratio is below 2:1 for all but the lowest mode, in which there are a few points above 3:1. It can be seen that this antenna would provide a fair match to 80 ohms over the four modes.

Table 3 is a condensation of the important features of a series of graphs similar to Figure 24. Tabulated is the average SWR for each mode with respect to R_{WM} for various values of Z_o and ψ.

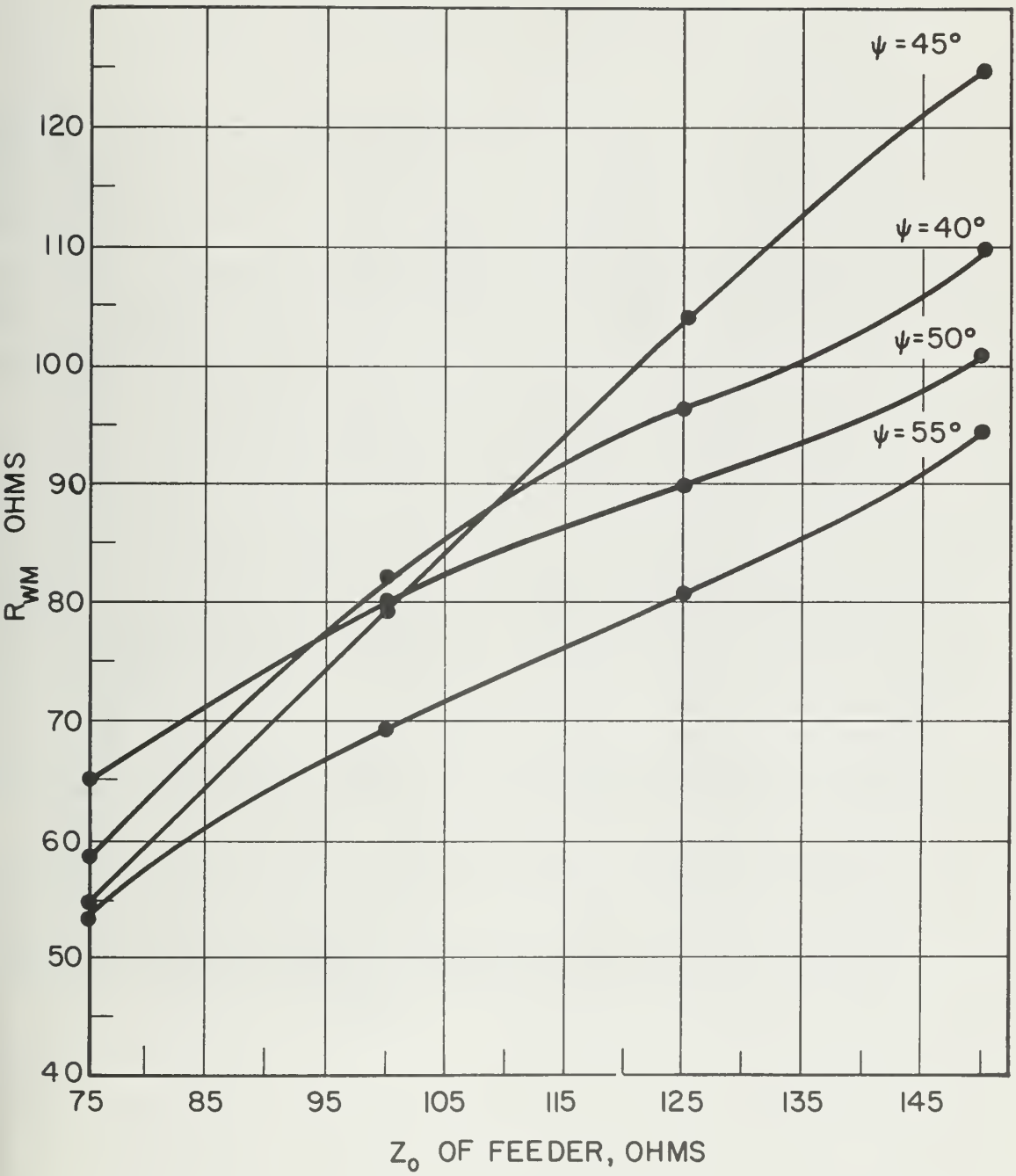

Figure 23. Weighted Mean Resistance Level R_{WM} vs. Characteristic Impedance of Feeder Z_o for Various Ψ Angles.

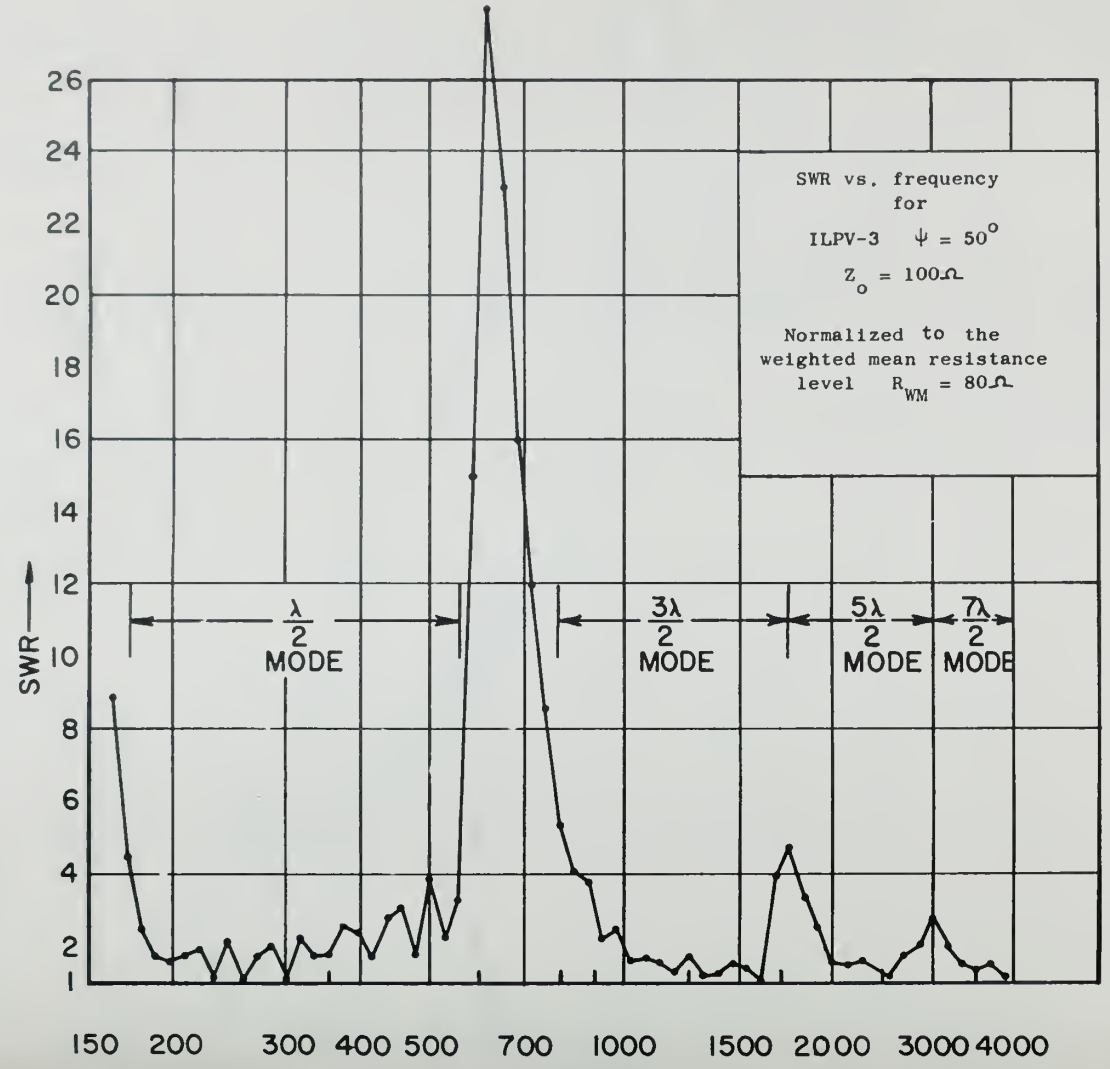
SWR vs. frequency
for
ILPV-3 ψ = 50°
Z_o = 100Ω
Normalized to the
weighted mean resistance
level R_WM = 80Ω
SWR
λ/2 MODE
3λ/2 MODE
5λ/2 MODE
7λ/2 MODE
26
24
22
20
18
16
14
12
10
8
6
4
2
1
150 200 300 400 500 700 1000 1500 2000 3000 4000
FREQUENCY, MCS.

FIGURE 24

TABLE 3

Table of values of average SWR with respect to R_{WM} for different Z_o and ψ.

ψ	Z_o	R_{WM}	Average SWR wrt R_{WM}			
			$\frac{\lambda}{2}$	$\frac{3\lambda}{2}$	$\frac{5\lambda}{2}$	$\frac{7\lambda}{2}$
40^o	75	58.2	1.6	1.5	1.6	1.6
	100	82.	1.8	1.4	1.5	1.6
	125	96.5	2.3	1.5	1.5	1.6
	150	110.	2.	1.7	2.3	3.
45^o	75	54.	1.8	1.8	1.8	2.
	100	79.4	1.6	1.6	1.7	1.7
	125	104.	2.4	1.5	1.4	1.8
	150	124.8	2.2	1.5	1.6	1.8
50^o	75	65.	1.9	1.6	1.5	1.5
	100	80.	1.9	1.6	1.6	1.6
	125	90.	1.9	1.5	1.6	1.6
	150	115.	2.	1.6	1.7	2.2
55^o	75	53.5	2 3	1 8	1 8	2
	100	69.3	2 4	1 7	1 7	1 8
	125	81.	2	1 6	1 6	2
	150	94.7	2 3	2 5	2 0	2 3

4. DESIGN CONSIDERATIONS FOR PARTICULAR APPLICATIONS

Several additional features of log-periodic dipole and V arrays have been briefly investigated as being of interest in some specialized applications.

4.1. Elimination of Central Elements

It is apparent from the preceding data that the resonant-V array is appropriate for use when it is desired to cover a number of discrete frequency bands which are widely distributed over the spectrum. Such frequency allocation are used in a number of commercial and government services. However, it is not often possible to fit the desired bands with a resonant-V array without some modification. One useful modification which has been proved feasible by measurement involves the elimination of some central elements from either the LP dipole or LPV array.

Since the coverage of any small frequency band is obtained from relatively few of the elements on the array, coverage of several adjacent bands may be obtained by retaining only the elements which are in the active region for those particular bands. Elements which on the ordinary dipole or V-array would contribute to the coverage of undesired portions of the spectrum can be simply removed and the remaining elements pushed together to shorten the over-all length of the array.

When using the resonant V array in higher modes, it is necessary to keep in mind that the elimination of central elements which may not be necessary in the $\lambda/2$ mode will also introduce holes in the coverage on the higher modes. Figure 25 shows a photograph of a pattern model LPV array designed to cover several bands with some central elements eliminated. Figure 26 shows the correspondence between elements on the antenna and frequency bands covered.

4.2 Off-Axis Beams

The principles of array design which have previously been applied to log-periodic elements[3] can also be applied to arrays of LPV elements to achieve even higher gain. Although further investigations of LPV elements with regard to position of phase center and methods of feed[2] are needed to aid in array design, one basic advantage of using LP resonant-V's as elements of larger arrays has been postulated and verified by a few measurement.

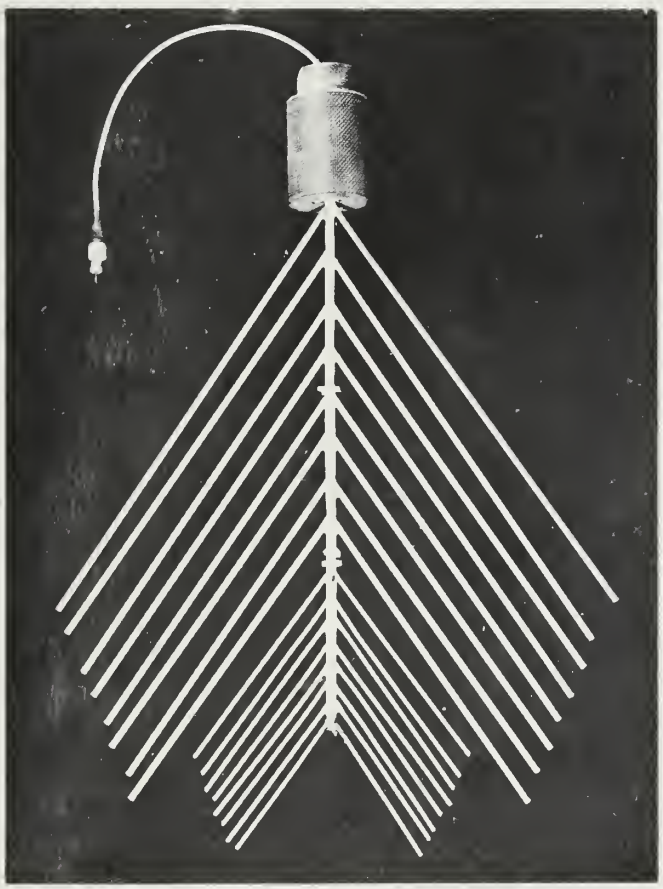

Figure 25. An LPV Array Showing Elimination of Central Elements to Tailor Design to Coverage of Desired Bands.

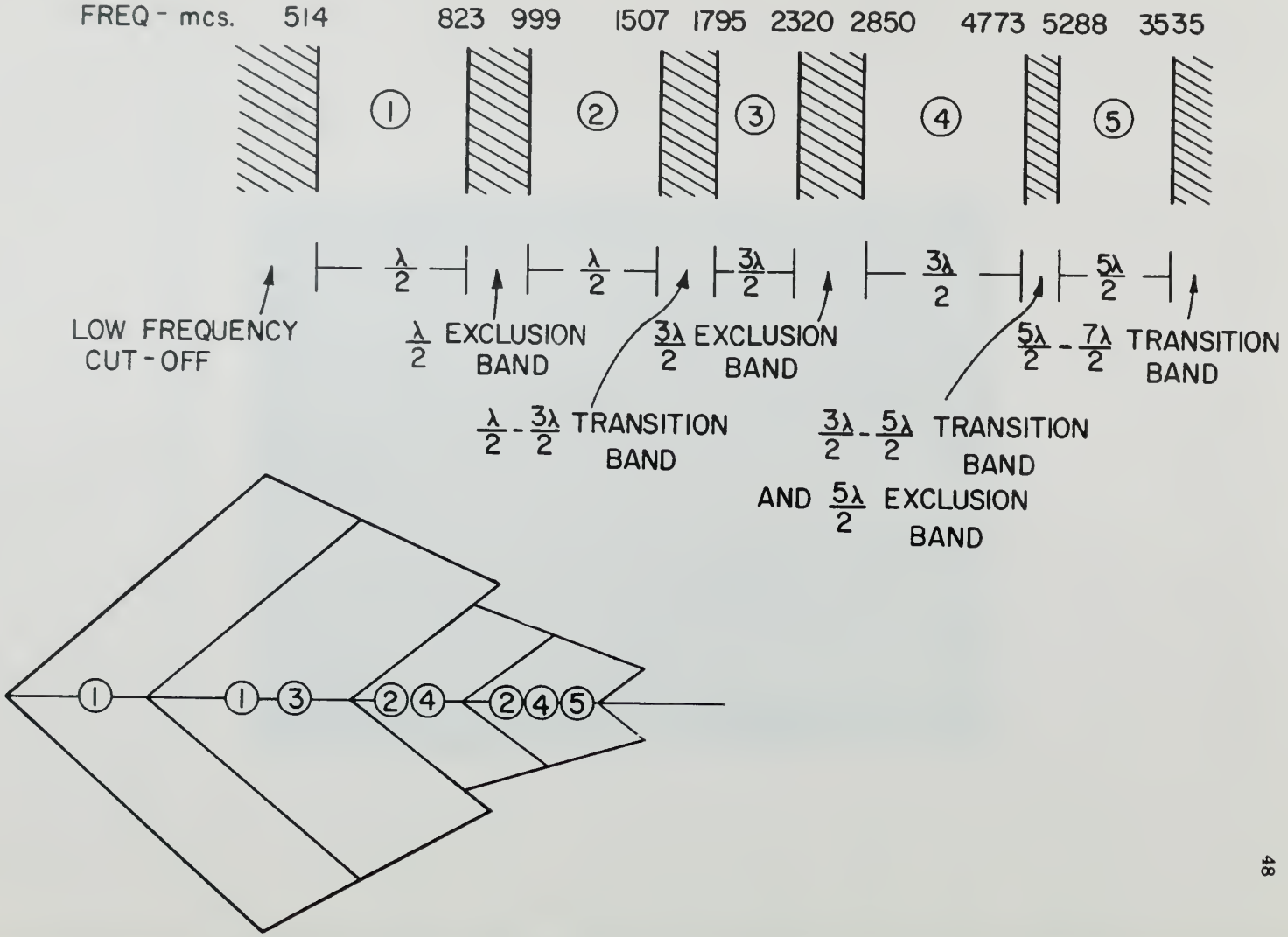

Figure 26. Frequency Bands Covered by Resonant-V Array with Some Central Elements Eliminated.

In order to maintain frequency independent performance in an array of LP elements, the phase centers of the elements should remain at a constant distance apart in terms of the wavelength. This is readily accomplished by feeding the LP elements from a common point as shown in Figure 27. With this method of feed, however, the direction of the axes of the several elements will vary. Using conventional end-fire elements, therefore, produces different element patterns because of the shift of the end-fire direction from element to element (see Figure 27).

In order to achieve maximum directive gain for an array of LP elements all of the elements of the array should have maximum directive gain in the same direction. Hence, the beam of each element should be tilted off-axis by the proper amount. Such a beam tilt can be achieved by simply tilting the elements relative to the feeder. Tilts in the E plane are produced in either the dipole array or the resonant-V array when the elements are aligned relative to the feeder as shown in Figure 28. Furthermore, a tilt in the H-plane can be achieved in the V array by tilting the elements as shown in Figure 29. In each of these cases the tilt of the beam is achieved by tilting the element pattern. The principal pattern characteristics are determined by the array factor and, aside from the pattern tilt, the patterns remain essentially the same as for the array with untilted elements.

The results of a few measurements of beam tilt are shown in Figures 30 and 31. In these curves the beam tilt was calculated by taking the average of the angles of the half-power points to locate the beam maximum. The deviation of this angle from the array axis of LPV-11 is plotted for several angles of tilt in Figure 30. Similar data for the H-plane are shown in Figure 31. The beam tilt is more pronounced in antennas with fairly large α since the element pattern in such cases is relatively more important in determining beam shape.

The beam tilt is not realized to a very great degree in the $\lambda/2$ mode since the elements themselves are not highly directive in this mode. A consistent beam tilt is observed in the higher modes and the data for these modes are shown in Figures 30 and 31.

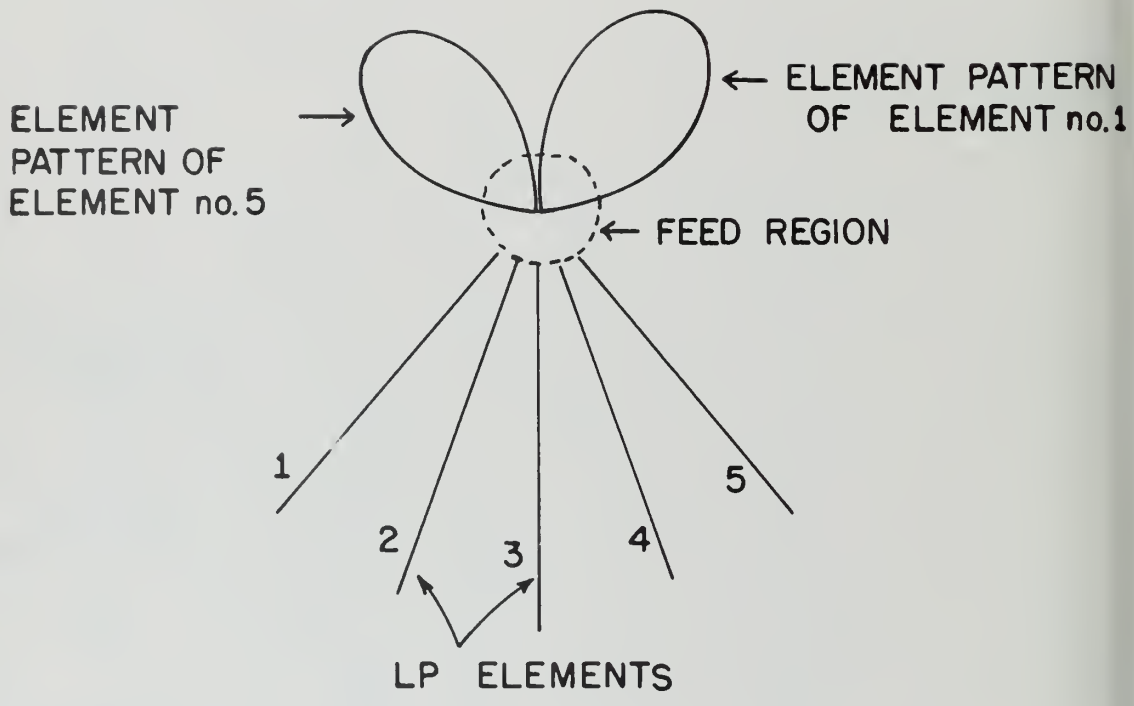

Figure 27. A Frequency Independent Array of Log-Periodic Elements.

(a)

LP DIPOLE ARRAY WITH ELEMENTS TILTED IN E – PLANE

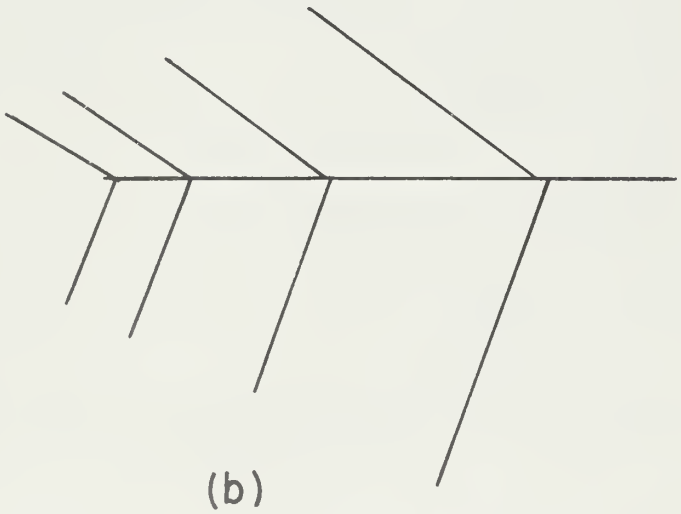

(b)

LPV ARRAY WITH ELEMENTS TILTED IN E – PLANE

Figure 28. Method of Tilting Elements in Dipole and V Arrays to Achieve Beam Tilt in E Plane.

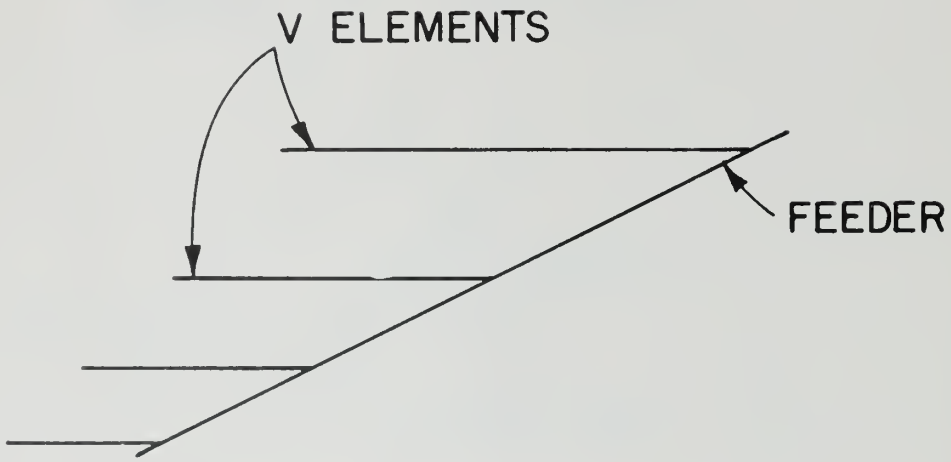

Figure 29. Method of Tilting Elements in V Array to Achieve Beam Tilt in H Plane

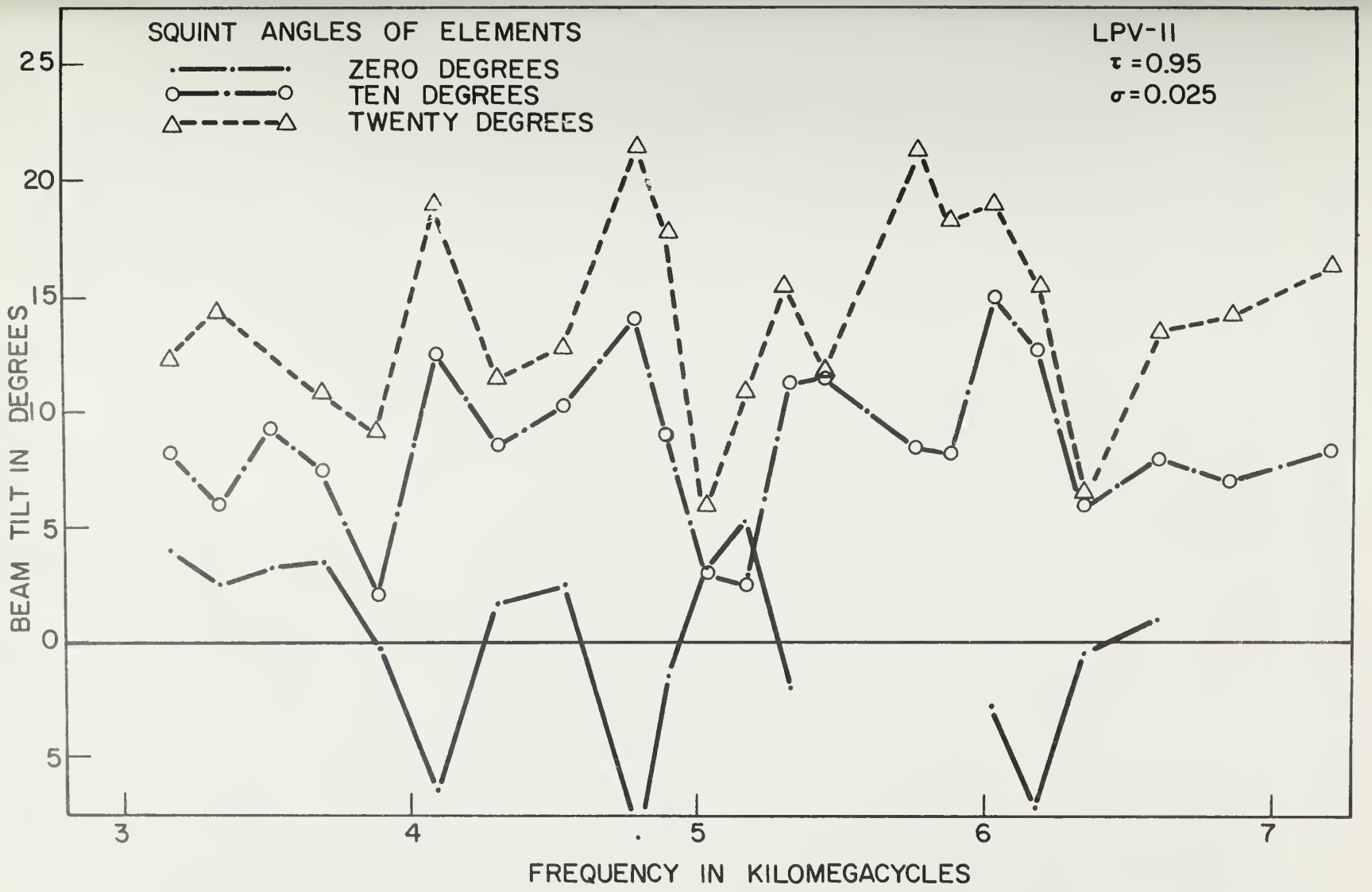

Figure 30. Beam Tilt Versus Frequency for Various Angles of Squint of V Elements in E-Plane.

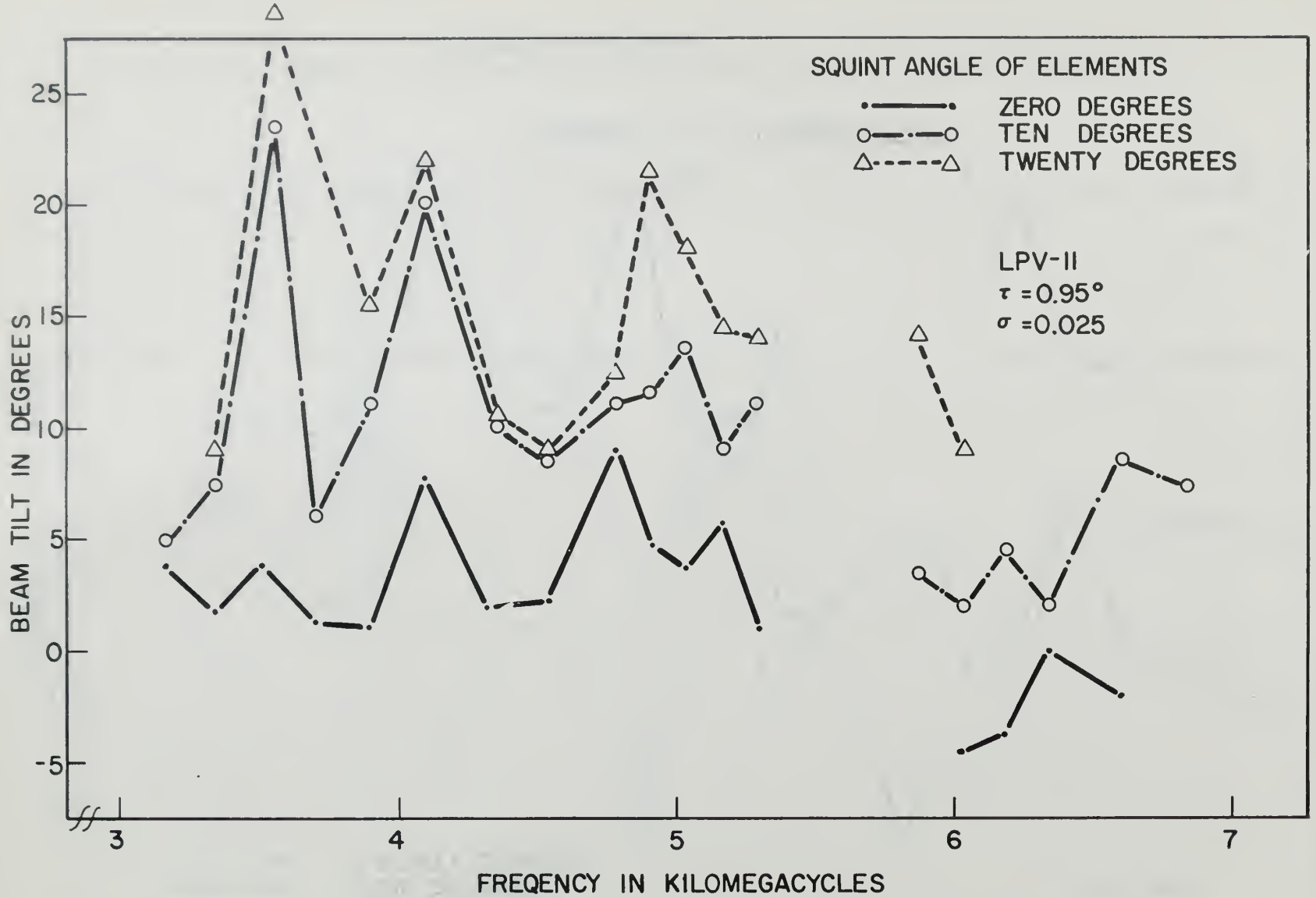

Figure 31. Beam Tilt Versus Frequency for Various Angles of Squint of V-Elements in H-Plane

5. CONCLUSIONS

It is obvious that a complete parameter study of the LPV arrays has not yet been accomplished. In any experimental investigation of wide band antennas one is confronted with the task of making thousands of measurements. The data reported here are drawn from hundreds of radiation patterns and over two thousand impedance measurements. Effort is now being directed towards making the experimental study by using a digital computer rather than laboratory models.

Enough data have been presented, however, to demonstrate the feasibility of the ideas expressed, to illustrate the validity of the general theory of operation, and to provide some data for practical designs. An important observation from the design viewpoint is the fact that the input impedance depends primarily upon the impedance of the feeder whereas the pattern depends primarily upon τ, σ, and ψ. This enables one to exercise somewhat independent control over the impedance and pattern over a limited range of parameters.

The LP resonant-V array provides essentially frequency-independent coverage of each of several frequency bands. In multi-mode operation, the characteristics change in a desirable way with frequency, achieving higher directive gain from the same physical structure as frequency increases. Antennas designed according to these concepts should find application whenever coverage of several widely dispersed frequency bands is desired.

REFERENCES

1. J. D. Dyson, "The Equiangular Spiral Antenna," IRE Trans. on Antennas and Propagation, Vol. AP-7, pp. 181-187, April, 1959. Technical Report No. 21, Contract No. AF 33(616)-3220, Antenna Lab., University of Illinois, Urbana, Illinois, September 1957.

2. J. D. Dyson, "The Unidirectional Equiangular Spiral Antenna," IRE. Trans., Vol. AP-7, October, 1959, pp. 329-334. Technical Report No. 33, Contract No. AF 33(616)-3220, Antenna Lab., University of Illinois, Urbana, Illinois, July 1958.

3. R. H. DuHamel & D. G. Berry, "Logarithmically Periodic Antenna Arrays," 1958 IRE Wescon Convention Records, Pt. I, pp. 161-174.

4. R. H. DuHamel & F. R. Ore, "Log-Periodic Feeds for Lens and Reflectors," 1959, IRE National Convention Record, Pt. I, pp. 128-137.

5. D. E. Isbell, "Log-Periodic Dipole Arrays," Technical Report No. 39, Contract No. AF 33(616)-6079, Antenna Lab., University of Illinois, Urbana, Illinois, June 1959. IRE Trans. on Antennas and Propagation, Vol. AP-8, pp. 260-267, May 1960.

6. J. A. Stratton, Electromagnetic Theory, McGraw-Hill, New York, N. Y. 1941, p. 488.

7. S. A. Schelkunoff & H. T. Friis, Antennas, Theory and Practice, John Wiley, New York, N. Y., 1952, p. 502.

8. J. D. Kraus, Antennas, McGraw-Hill, New York, N. Y., 1950, p. 25.

ANTENNA LABORATORY
TECHNICAL REPORTS AND MEMORANDA ISSUED

Contract AF33(616)-310

"Synthesis of Aperture Antennas," Technical Report No. 1, C.T.A. Johnk, October, 1954.*

"A Synthesis Method for Broad-band Antenna Impedance Matching Networks," Technical Report No. 2, Nicholas Yaru, 1 February 1955.*

"The Asymmetrically Excited Spherical Antenna," Technical Report No. 3, Robert C. Hansen, 30 April 1955.*

"Analysis of an Airborne Homing System," Technical Report No. 4, Paul E. Mayes, 1 June 1955 (CONFIDENTIAL).

"Coupling of Antenna Elements to a Circular Surface Waveguide," Technical Report No. 5, H. E. King and R. H. DuHamel, 30 June 1955.*

"Axially Excited Surface Wave Antennas," Technical Report No. 7, D. E. Royal, 10 October 1955.*

"Homing Antennas for the F-86F Aircraft (450-2500mc)," Technical Report No. 8, P.E. Mayes, R.F. Hyneman, and R.C. Becker, 20 February 1957, (CONFIDENTIAL).

"Ground Screen Pattern Range," Technical Memorandum No. 1, Roger R. Trapp, 10 July 1955.*

Contract AF33(616)-3220

"Effective Permeability of Spheroidal Shells," Technical Report No. 9, E. J. Scott and R. H. DuHamel, 16 April 1956.

"An Analytical Study of Spaced Loop ADF Antenna Systems," Technical Report No. 10, D. G. Berry and J. B. Kreer, 10 May 1956.

"A Technique for Controlling the Radiation from Dielectric Rod Waveguides," Technical Report No. 11, J. W. Duncan and R. H. DuHamel, 15 July 1956.*

"Directional Characteristics of a U-Shaped Slot Antenna," Technical Report No. 12, Richard C. Becker, 30 September 1956.**

"Impedance of Ferrite Loop Antennas," Technical Report No. 13, V. H. Rumsey and W. L. Weeks, 15 October 1956.

"Closely Spaced Transverse Slots in Rectangular Waveguide," Technical Report No. 14, Richard F. Hyneman, 20 December 1956.

"Distributed Coupling to Surface Wave Antennas," Technical Report No. 15, Ralph Richard Hodges, Jr., 5 January 1957.**

"The Characteristic Impedance of the Fin Antenna of Infinite Length," Technical Report No. 16, Robert L. Carrel, 15 January 1957.*

"On the Estimation of Ferrite Loop Antenna Impedance," Technical Report No. 17, Walter L. Weeks, 10 April 1957.*

"A Note Concerning a Mechanical Scanning System for a Flush Mounted Line Source Antenna," Technical Report No. 18, Walter L. Weeks, 20 April 1957.

"Broadband Logarithmically Periodic Antenna Structures," Technical Report No. 19, R. H. DuHamel and D. E. Isbell, 1 May 1957.

"Frequency Independent Antennas," Technical Report No. 20, V. H. Rumsey, 25 October 1957.

"The Equiangular Spiral Antenna," Technical Report No. 21, J. D. Dyson, 15 September 1957.

"Experimental Investigation of the Conical Spiral Antenna," Technical Report No. 22, R. L. Carrel, 25 May 1957.**

"Coupling between a Parallel Plate Waveguide and a Surface Waveguide," Technical Report No. 23, E. J. Scott, 10 August 1957.

"Launching Efficiency of Wires and Slots for a Dielectric Rod Waveguide," Technical Report No. 24, J. W. Duncan and R. H. DuHamel, August 1957.

"The Characteristic Impedance of an Infinite Biconical Antenna of Arbitrary Cross Section," Technical Report No. 25, Robert L. Carrel, August 1957.

"Cavity-Backed Slot Antennas," Technical Report No. 26, R. J. Tector, 30 October 1957.

"Coupled Waveguide Excitation of Traveling Wave Slot Antennas," Technical Report No. 27, W. L. Weeks, 1 December 1957.

"Phase Velocities in Rectangular Waveguide Partially Filled with Dielectric," Technical Report No. 28, W. L. Weeks, 20 December 1957.

"Measuring the Capacitance per Unit Length of Biconical Structures of Arbitrary Cross Section," Technical Report No. 29, J. D. Dyson, 10 January 1958.

"Non-Planar Logarithmically Periodic Antenna Structure," Technical Report No. 30, D. W. Isbell, 20 February 1958.

"Electromagnetic Fields in Rectangular Slots," Technical Report No. 31, N. J. Kuhn and P. E. Mast, 10 March 1958.

"The Efficiency of Excitation of a Surface Wave on a Dielectric Cylinder," Technical Report No. 32, J. W. Duncan, 25 May 1958.

"A Unidirectional Equiangular Spiral Antenna," Technical Report No. 33, J. D. Dyson, 10 July 1958.

"Dielectric Coated Spheroidal Radiators," Technical Report No. 34, W. L. Weeks, 12 September 1958.

"A Theoretical Study of the Equiangular Spiral Antenna," Technical Report No. 35, P. E. Mast, 12 September 1958.

Contract AF33(616)-6079

"Use of Coupled Waveguides in a Traveling Wave Scanning Antenna," Technical Report No. 36, R. H. MacPhie, 30 April 1959.

"On the Solution of a Class of Wiener-Hopf Integral Equations in Finite and Infinite Ranges," Technical Report No. 37, Raj Mittra, 15 May 1959.

"Prolate Spheroidal Wave Functions for Electromagnetic Theory," Technical Report No. 38, W. L. Weeks, 5 June 1959.

"Log Periodic Dipole Arrays," Technical Report No. 39, D.E. Isbell, 1 June 1959.

"A Study of the Coma-Corrected Zoned Mirror by Diffraction Theory," Technical Report No. 40, S. Dasgupta and Y. T. Lo, 17 July 1959.

"The Radiation Pattern of a Dipole on a Finite Dielectric Sheet," Technical Report No. 41, K. G. Balmain, 1 August 1959.

"The Finite Range Wiener-Hopf Integral Equation and a Boundary Value Problem in a Waveguide," Technical Report No. 42, Raj Mittra, 1 October 1959.

"Impedance Properties of Complementary Multiterminal Planar Structures," Technical Report No. 43, G. A. Deschamps, 11 November 1959.

"On the Synthesis of Strip Sources," Technical Report No. 44, Raj Mittra, 4 December 1959.

"Numerical Analysis of the Eigenvalue Problem of Waves in Cylindrical Waveguides," Technical Report No. 45, C. H. Tang and Y. T. Lo, 11 March 1960.

"New Circularly Polarized Frequency Independent Antennas With Conical Beam or Omnidirectional Patterns," Technical Report No. 46, J.D.Dyson and P.E. Mayes, 20 June 1960.

"Logarithmically Periodic Resonant-V Arrays," Technical Report No. 47, P.E. Mayes and R. L. Carrel, 15 July 1960.

---

* Copies available for a three week loan period.

** Copies no longer available.

AF 33(616) -6079

DISTRIBUTION LIST

One copy each unless otherwise indicated

Commander
Wright Air Development Center
Attn: WCOSI, Library
Wright-Patterson Air Force Base, Ohio

Commander
U.S. Naval Air Test Center
Attn: ET-315, Antenna Section
Patuxent River, Maryland

Chief
Bureau Naval Weapons
Department of the Navy
Attn: (RR-13)
Washington 25, D.C.

Commander
Air Force Missile Test Center
Attn: Technical Library
Patrick Air Force Base, Florida

Director
Ballistics Research Lab.
Attn: Ballistics Measurement Lab.
Aberdeen Proving Ground, Maryland

Office of the Chief Signal Officer
Attn: SIGNET-5
Eng. & Technical Division
Washington 25, D.C.

National Bureau of Standards
Department of Commerce
Attn: Dr. A. G. McNish
Washington 25, D.C.

Director
U.S. Navy Electronics Lab.
Point Loma
San Diego 52, California

*Wright Air Development Division
Attn: N.C. Draganjac, WWDBEG
Wright-Patterson AFB, Ohio (2 copies)

Commander
USA White Sands Signal Agency
White Sands Proving Command
Attn: SIGWS-FC-02
White Sands, New Mexico

Director
Air University Library
Attn: AUL-8489
Maxwell AFB, Alabama

Army Rocket and Guided Missile Agency
U.S. Army Ordnance Missile Agency
Attn: ORDXR-OMR
Redstone Arsenal, Alabama

Commander
Aero Space Technical Intelligence Center
Attn: AFCIN-4c3b, Mr. Lee Roy Hay
Wright-Patterson AFB, Ohio

Commander
801st Air Division (SAC)
Attn: DCTT, Major Witry
Lockbourne Air Force Base, Ohio

Director
Air University Library
Attn: AUL-9642
Maxwell Air Force Base, Alabama

Chief
Bureau of Aeronautics
Attn: Aer-EL-931
Department of the Navy
Washington 25, D.C.

Armed Services Technical Information Agency
ATTN: TIP-DR
Arlington Hall Station
Arlington 12, Virginia (10 copies)
(Excluding Top Secret and Restricted Data)(Reference AFR 205-43)

Commander
Wright Air Development Center
Attn: F. Behrens, WCLKR
Wright-Patterson AFB, Ohio

Commander
Air Research & Development Command
Attn: RDTC
Andrews Air Force Base
Washington 25, D.C.

Commander
Hq. Air Force Cambridge Research Center
ATTN: CRRD, C. Sletten
Laurence G. Hanscom Field
Bedford, Massachusetts

Commander
Air Proving Ground Command
Attn: Classified Technical Data
Branch D/OI
Eglin Air Force Base, Florida

Director
Research and Development Command
Hq. USAF
Attn: AFDRD-RE
Washington 25, D.C.

Commander
Air Force Ballistics Missile Division
Attn: Technical Library
Air Force Unit Post Office
Los Angeles 45, California

Commander
Air Force Missile Development Center
Attn: Technical Library
Holloman Air Force Base, New Mexico

Commander
801st Air Division (SAC)
Attn: DCTTTD, Major Hougan
Lockbourne Air Force Base, Ohio

Commander
Rome Air Development Center
Attn: RCERA-1, M. Diab
Griffiss Air Force Base, New York

Director
Naval Research Laboratory
Attn: Dr. A. Marston
Anacostia
Washington 25, D.C.

Director, Surveillance Dept.
Evans Area
Attn: Technical Document Center
Belmar, New Jersey

Chief, Bureau of Ships
Department of the Navy
Attn: Code 838D
Washington 25, D.C.

Commanding Officer & Director
U.S. Navy Electronics Laboratory
Attn: Library
San Diego 52, California

Andrew Alford Consulting Engineers
Attn: Dr. A. Alford
M/F Contract AF33(600)-36108
299 Atlantic Avenue
Boston 10, Massachusetts

ATA Corporation
1200 Duke Street
Alexandria, Virginia

Bell Telephone Labs., Inc.
Attn: R. L. Mattingly
M/F Contract AF33(616)-5499
Whippany, New Jersey

Bendix Radio Division
Bendix Aviation Corporation
Attn: Dr. K. F. Umpleby
M/F Contract AF33(600)-35407
Towson 4, Maryland

Boeing Airplane Company
Attn: C. Armstrong
M/F Contract AF33(600)-36319
7755 Marginal Way
Seattle, Washington

Boeing Airplane Company
Attn: Robert Shannon
M/F Contract AF33(600)-35992
Wichita, Kansas

Canoga Corporation
M/F Contract AF08(603)-4327
5955 Sepulveda Boulevard
P.O. Box 550
Van Nuys, California

Dr. C. H. Papas
Department of Electrical Engineering
California Institute of Technology
Pasadena, California

Chance-Vought Aircraft Division
United Aircraft Corporation
Attn: R.C. Blaylock
THRU: BuAer Representative
M/F Contract NOa(s) 57-187
Dallas, Texas

Collins Radio Company
Attn: Dr. R. H. DuHamel
M/F Contract AF33(600)-37559
Cedar Rapids, Iowa

CONVAIR
Attn: R. Honer
M/F Contract AF33(600)-26530
San Diego Division
San Diego 12, California

CONVAIR
Fort Worth Division
Attn: C. R. Curnutt
M/F Contract AF33(600)-32841 &
AF33(600)-31625
Fort Worth, Texas

Department of Electrical Engineering
Attn: Dr. H. G. Booker
Cornell University
Ithaca, New York

University of Denver
Denver Research Institute
University Park
Denver 10, Colorado

Dalmo Victor Company
Attn: Engineering Technical Library
M/F Contract AF33(600)-27570
1515 Industrial Way
Belmont, California

Dorne & Margolin, Inc.
M/F Contract AF33(600)-35992
30 Sylvester Street
Westbury
Long Island, New York

Douglas Aircraft Co., Inc.
Attn: G. O'Rilley
M/F Contract AF33(600)-25669 &
AF33(600)-28368
Tulsa, Oklahoma

Exchange and Gift Division
The Library of Congress
Washington 25, D.C. (2 copies)

Fairchild Engine & Airplane Corp.
Fairchild Aircraft Division
Attn: Engineering Library
S. Rolfe Gregory
M/F Contract AF33(038)-18499
Hagerstown, Maryland

Dr. Frank Fu Fang
Boeing Airplane Company
Transport Division, Physical Research
Renton, Washington

General Electric Company
Attn: D. H. Kuhn, Electronics Lab.
M/F Contract AF30(635)-12720
Building 3, Room 301
College Park
113 S. Salina Street
Syracuse, New York

General Electronic Laboratories, Inc.
Attn: F. Parisi
M/F Contract AF33(600)-35796
18 Ames Street
Cambridge 42, Massachusetts

Goodyear Aircraft Corporation
Attn: G. Welch
M/F Contract AF33(616)-5017
Akron, Ohio

Granger Associates
M/F Contract AF19(604)-5509
966 Commercial Street
Palo Alto, California

Grumman Aircraft Engineering Corp.
Attn: J. S. Erickson
Asst. Chief, Avionics Dept.
M/F Contract NOa(s) 51-118
Bethpage, Long Island, New York

Gulton Industries, Inc.
Attn: B. Bittner
M/F Contract AF33(600)-36869
P.O. Box 8345
15000 Central, East
Albuquerque, New Mexico

Hallicrafters Corporation
Attn: D. Herling
M/F Contract AF33(604)-21260
440 W. Fifth Avenue
Chicago, Illinois

Technical Reports Collection
Attn: Mrs. E. L. Hufschmidt
Librarian
303 A. Pierce Hall
Harvard University
Cambridge 38, Massachusetts

Hoffman Laboratories, Inc.
Attn: S. Varian (for Classified)
Technical Library (for Unclassified)
M/F Contract AF33(604)-17231
Los Angeles, California

Dr. R. F. Hyneman
P.O. Box 2097
Mail Station C-152
Building 600
Hughes Ground Systems Group
Fullerton, California

HRB-Singer, Inc.
Attn: Mr. R. A. Evans
Science Park
State College, Pa.

Mr. Dwight Isbell
4620 Sunnyside
Seattle 3, Washington

ITT Laboratories
Attn: A. Kandoian
M/F Contract AF33(616)-5120
500 Washington Avenue
Nutley 10, New Jersey

ITT Laboratories
Attn: L. DeRosa
M/F Contract AF33(616)-5120
500 Washington Avenue
Nutley 10, New Jersey

ITT Laboratories
A Div. of Int. Tel. & Tel. Corp.
Attn: G. S. Giffin, ECM Lab.
3700 E. Pontiac Street
Fort Wayne, Indiana

Jansky and Bailey, Inc.
Engineering Building
Attn: Mr. D. C. Ports
1339 Wisconsin Avenue, N.W.
Washington, D.C.

Jasik Laboratories, Inc.
100 Shames Drive
Westbury, New York

John Hopkins University
Radiation Laboratory
Attn: Librarian
M/F Contract AF33(616)-68
1315 St. Paul Street
Baltimore 2, Maryland

Applied Physics Laboratory
Johns Hopkins University
8621 Georgia Avenue
Silver Spring, Maryland

Lincoln Laboratories
Attn: Document Room
M/F Contract AF19(122)-458
Massachusetts Institute of Technology
P.O. Box 73
Lexington 73, Massachusetts

Litton Industries, Inc.
Maryland Division
Attn: Engineering Library
M/F Contract AF33(600)-37292
4900 Calvert Road
College Park, Maryland

Lockheed Aircraft Corporation
Attn: C. D. Johnson
M/F Contract NOa(s) 55-172
P.O. Box 55
Burbank, California

Lockheed Missiles & Space Division
Attn: E. A. Blasi
M/F Contract AF33(600)-28692 &
AF33(616)-6022
Department 58-15
Plant 1, Building 130
Sunnyvale, California

The Martin Company
Attn: W. A. Kee, Chief Librarian
M/F Contract AF33(600)-37705
Library & Document Section
Baltimore 3, Maryland

Ennis Kuhlman
McDonnell Aircraft
P.O. Box 516
Lambert Municipal Airport
St. Louis 21, Missouri

Melpar, Inc.
Attn: Technical Library
M/F Contract AF19(604)-4988
Antenna Laboratory
3000 Arlington Blvd.
Falls Church, Virginia

Melville Laboratories
Walt Whitman Road
Melville, Long Island,
New York

University of Michigan
Aeronautical Research Center
Attn: Dr. K. Seigel
M/F Contract AF30(602)-1853
Willow Run Airport
Ypsilanti, Michigan

Microwave Radiation Co., Inc.
Attn: Dr. M. J. Ehrlich
M/F Contract AF33(616)-6528
19223 S. Hamilton Street
Gardena, California

Motorola, Inc.
Attn: R. C. Huntington
8201 E. McDowell Road
Phoenix, Arizona

Physical Science Lab.
Attn: R. Dressel
New Mexico College of A and MA
State College, New Mexico

North American Aviation, Inc.
Attn: J. D. Leonard, Eng. Dept.
M/F Contract NOa(s) 54-323
4300 E. Fifth Avenue
Columbus, Ohio

North American Aviation, Inc.
Attn: H. A. Storms
M/F Contract AF33(600)-36599
Department 56
International Airport
Los Angeles 45, California

Northrop Aircraft, Inc.
Attn: Northrop Library, Dept. 2135
M/F Contract AF33 (600)-27679
Hawthorne, California

Dr. R. E. Beam
Microwave Laboratory
Northwestern University
Evanston, Illinois

Ohio State University Research
Foundation
Attn: Dr. T. C. Tice
M/F Contract AF33(616)-6211
1314 Kinnear Road
Columbus 8, Ohio

University of Oklahoma Res. Inst.
Attn: Prof. C. L. Farrar
M/F Contract AF33(616)-5490
Norman, Oklahoma

Philco Corporation
Government and Industrial Division
Attn: Dr. Koehler
M/F Contract AF33(616)-5325
4700 Wissachickon Avenue
Philadelphia 44, Pennsylvania

Prof. A. A. Oliner
Microwave Research Institute
Polytechnic Institute of Brooklyn
55 Johnson Street - Third Floor
Brooklyn, New York

Radiation, Inc.
Technical Library Section
Attn: Antenna Department
M/F Contract AF33(600)-36705
Melbourne, Florida

Radio Corporation of America
RCA Laboratories Division
Attn: Librarian
M/F Contract AF33(616)-3920
Princeton, New Jersey

Radioplane Company
M/F Contract AF33(600)-23893
Van Nuys, California

Ramo-Wooldridge, a division of
Thompson Ramo Wooldridge, Inc.
Attn: Technical Information Services
8433 Fallbrook Avenue
P.O. Box 1006
Canoga Park, California

Dr. D. E. Royal
Ramo-Wooldridge, a division of Thompson
Ramo Wooldridge Inc.
8433 Fallbrook Avenue
Canoga Park, California

Rand Corporation
Attn: Librarian
M/F Contract AF18(600)-1600
1700 Main Street
Santa Monica, California

Rantec Corporation
Attn: R. Krausz
M/F Contract AF19(604)-3467
Calabasas, California

Raytheon Manufacturing Corp.
Attn: Dr. R. Borts
M/F Contract AF33(604)-15634
Wayland, Massachusetts

Republic Aviation Corporation
Attn: Engineering Library
M/F Contract AF33(600)-34752
Farmingdale
Long Island, New York

Republic Aviation Corporation
Guided Missiles Division
Attn: J. Shea
M/F Contract AF33(616)-5925
223 Jericho Turnpike
Mineola, Long Island, New York

Sanders Associates, Inc.
95 Canal Street
Attn: Technical Library
Nashua, New Hampshire

Smyth Research Associates
Attn: J. B. Smyth
3555 Aero Court
San Diego 11, California

Space Technology Labs, Inc.
Attn: Dr. R. C. Hansen
P.O. Box 95001
Los Angeles 45, California
M/F Contract AF04(647)-361

Sperry Gyroscope Company
Attn: B. Berkowitz
M/F Contract AF33(600)-28107
Great Neck
Long Island, New York

Stanford Electronics Laboratory
Attn: Applied Electronics Lab.
Document Library
Stanford University
Stanford, California

Stanford Research Institute
Attn: Mary Lou Fields, Acquisitions
Documents Center
Menlo Park, California

Stanford Research Institute
Aircraft Radiation Systems Lab.
Attn: D. Scheuch
M/F Contract AF33(616)-5584
Menlo Park, California

Sylvania Electric Products, Inc.
Electronic Defense Laboratory
M/F Contract DA 36-039-SC-75012
P.O. Box 205
Mountain View, California

Mr. Roger Battie
Supervisor, Technical Liaison
Sylvania Electric Products, Inc.
Electronic Systems Division
P.O. Box 188
Mountain View, California

Sylvania Electric Products, Inc.
Electric Systems Division
Attn: C. Faflick
M/F Contract AF33(038)-21250
100 First Street
Waltham 54, Massachusetts

Tamar Electronics, Inc.
Attn: L.B. McMurren
2045 W. Rosecrans Avenue
Gardena, California

Technical Research Group
M/F Contract AF33(616)-6093
2 Aerial Way
Syosset, New York

Temco Aircraft Corporation
Attn: G. Cramer
M/F Contract AF33(600)-36145
Garland, Texas

Electrical Engineering Res. Lab.
University of Texas
Box 8026, University Station
Austin, Texas

A. S. Thomas, Inc.
M/F Contract AF04(645)-30
161 Devonshire Street
Boston 10, Massachusetts

Westinghouse Electric Corporation
Air Arm Division
Attn: P. D. Newhouser
Development Engineering
M/F Contract AF33(600)-27852
Friendship Airport
Baltimore, Maryland

Professor Morris Kline
Institute of Mathematical Sciences
New York University
25 Waverly Place
New York 3, New York

Dr. S. Dasgupta
Government Engineering College
Jabalpur, M.P.
India

Dr. Richard C. Becker
10829 Berkshire
Westchester, Illinois

The Engineering Library
Princeton University
Princeton, New Jersey

Dr. B. Chatterjee
Communication Engineering Dept.
Indian Institute of Technology
Kharagpur (S.E. Rly.)
India

Sperry Phoenix Company
Attn: Technical Librarian
P.O. Box 2529
21111 North 19th Avenue
Phoenix, Arizonia

Dr. Harry Letaw, Jr.
Raytheon Company
Surface Radar and Navigation Operations
State Road West
Wayland, Massachusetts